Deutsches Zentrum
für Luft- und Raumfahrt
Institut für
Vernetzte Energiesysteme

Chair of Technical
Thermodynamics

RWTH AACHEN
UNIVERSITY

The present work was submitted to Chair of Technical Thermodynamics

Spatially and temporally resolved potential analysis and allocation optimization of power-to-gas plants in Germany

Master's Thesis

by
Nils Neuland

1^{st} Examiner: Prof. Dr.-Ing. Dipl.-Wirt.Ing. Niklas von der Aßen
2^{nd} Examiner: Andreas Kämper, M.Sc.

Internal Supervisor: Yifan Wang, M.Sc.,
External Supervisor: Wilko Heitkötter, M.Sc., German Aerospace Center (DLR), Institute of Networked Energy Systems

Aachen, January 20, 2021

Abstract

In order to meet emission reduction target, the energy system transitions into higher shares of renewable energy sources (RES) and the use of conventional power plants is reduced. The rising share of RES increases the demand for flexibility options in the power grid. Power-to-gas plants are a much-discussed option that could provide the power grid with flexibility. Power-to-gas plants can be operated with surplus electricity to feed hydrogen and methane into the gas grid. In this way, power-to-gas plants contribute to the avoidance of congestions in the electricity grid. Since power-to-gas plants are intended to feed into the gas grid, the storage capacity of the gas grid represents a limiting factor for allocating power-to-gas plants.

The aim of this work is to determine the spatially and temporally resolved installable capacity of power-to-gas plants at the level of medium voltage (MV) Grid Districts. The installable capacity is calculated separately for the gas transmission grid and the gas distribution grid. Regionalization methods and load profiles are used to spatially and temporally resolve the installable capacity. The potential for feeding hydrogen and methane into the gas grid is determined in order to allow optimizations for the allocation of power-to-hydrogen plants and power-to-methane plants.

The integration of the installable capacity into the power grid model electricity Transmission Grid optimization (eTraGo) allows an optimization of the allocation of the power-to-gas plants considering the gas grid. The three research questions investigated are: how does the spatial distribution of the installable capacity of power-to-gas plants affect the allocation of power-to-gas plants, how does the temporal distribution of the installable capacity of power-to-gas plants influence the allocation of power-to-gas plants, and what is the impact of the maximum permitted concentration of hydrogen in the gas grid on the allocation of power-to-gas plants.

The research questions are answered using six optimization cases. To determine the temporal influence, calculations are carried out for different periods of the year as well as for the entire year. Optimizations are performed with different permitted concentration of hydrogen in the gas grid to determine their impact on the allocation. The influence of the spatial distribution of the installable capacity of power-to-gas plants is investigated using all six optimization cases.

The installable capacity of power-to-gas plants per MV Grid District strongly depends on whether the district includes only the gas distribution grid or also the transmission grid. The installable capacity of power-to-hydrogen plants feeding into the transmission grid is on average 860 MW_{el} per MV Grid District. But the installable capacity of power-to-hydrogen plants feeding into the distribution grid is on average 1.5 MW_{el}. The same applies to power-to-methane plants. Therefore, the plants are mainly built for feeding into the transmission grid. Increasing the maximum allowed hydrogen concentration in the gas grid results in fewer but larger plants built. In summary, the determined installable capacity of power-to-gas plants feeding into the gas grid can be used to determine an optimal allocation of power-to-gas plants taking into account the gas grid.

Contents

List of Figures

List of Tables

List of Abbreviations

CHP combined heat and power
eDisGo electricity Distribution Grid optimization
eGo electricity Grid optimization
EHV extra high voltage
eTraGo electricity Transmission Grid optimization
GHG greenhouse gas
GVA gross value added
HV high voltage
LHV lower heating value
LKD-EU Long-term planning and short-term optimization of the German electricity system within the European framework
LOHC liquid organic hydrogen carriers
LOPF linear optimal power flow
LV low voltage
MV medium voltage
OEDB OpenEnergyDatabase
RES renewable energy sources
OEP OpenEnergyPlatform
ORC organic rankine cycle
PEM proton exchange membrane
PtG power-to-gas
PyPSA Python for Power System Analysis
TSO transmission system operator

1 Motivation

Climate change is one of the major challenges of our times. Due to human-induced global warming, the global mean temperature reached approximately 1 °C above the pre-industrial global mean temperature in 2017 and is increasing at 0.2 °C per decade [10]. At the climate conference in Paris 197 countries agreed on limiting the increasing global mean temperature to well below 2 °C above pre-industrial levels [11]. To achieve this, emissions of greenhouse gases (GHGs) must be reduced.

GHG emissions can be minimized by transforming the fossil fuel-based energy system into a sustainable energy system without fossil fuels. The fossil fuels are substituted by an increasing share of RES. In Germany, RES have a share of 17.1 % of the final energy consumption in 2019 [12]. The federal government's target is to increase the share of RES in final energy consumption by 60 % until 2050 [13].

The introduction of renewable energies has progressed differently in the sectors of electricity, heat and mobility. Looking at the electricity sector more in detail, the share of power produced by RES increased over the past 18 years, as shown in Figure 1.1. The rising share of RES such as wind turbines and photovoltaic systems increases the measures for regulating the electricity grid. While in 2010 redispatch measures for 306 GW h were required, in 2017 over 20 000 GW h needed to be redispatched to eliminate network bottlenecks [14]. Also when looking at the curtailment of RES it becomes apparent that due to a rising share of RES a flexible electricity grid is required. In 2019, over 6000 GW h of power generated by RES had to be curtailed [15], and it is estimated to increase up to 12 000 GW h by 2030 [16]. The federal government plans to expand the use of RES so that 80 % of electricity is produced from RES in 2050 [13]. The integration of RES into the sectors of heat and mobility is currently not as progressed as in the electricity sector. The share of RES of final energy consumption reached in electricity sector 42.1 %, heat 14.5 % and mobility 5.6 % in 2019 [12]. Due to these differences, the potential of saving GHG emissions and decarbonizing in the sectors heat and mobility is higher than in the electricity sector.

The more volatile RES are added to the energy system the more flexibility is required in

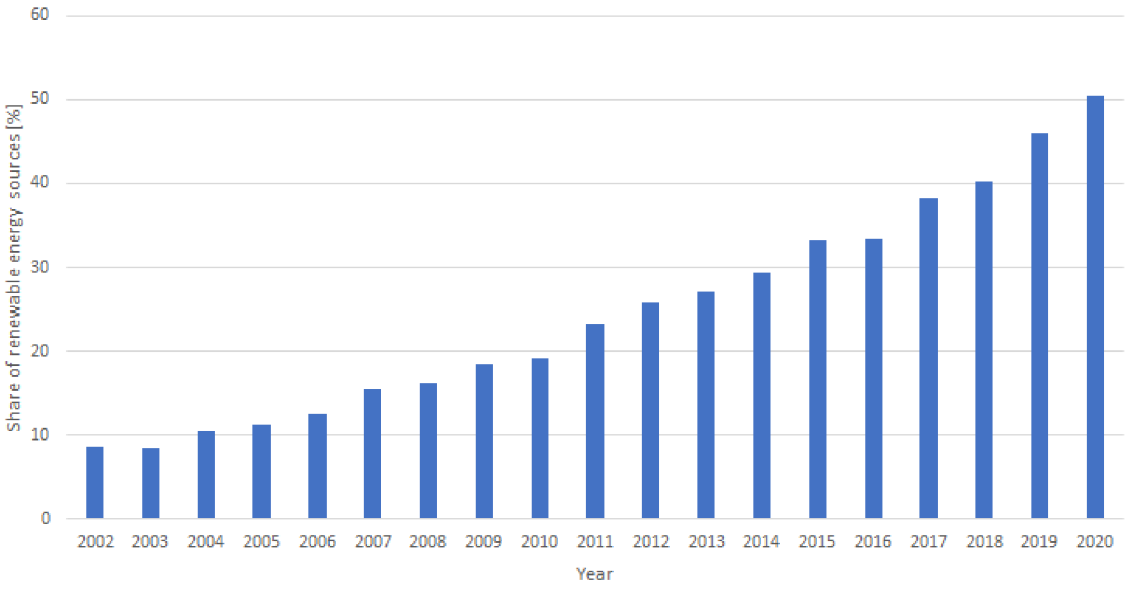

Figure 1.1: Annual share of renewable energy sources in electricity generation in Germany [1]

the electricity grid. To ensure this, several options are available such as conversion and expansion of the power grid, additional energy storage facilities, demand side management and measures on the generation side [17].

A much-discussed measure for providing flexibility to the electricity grid is sector coupling. Sector coupling is the networking of the electricity, heat, mobility and industry sector. The sectors are no longer considered separately, but optimized as part of the overall system. Figure 1.2 shows the principle of sector coupling [2]. Power generated from RES is used to decarbonize the industry, residential and transport sector. In the process, electricity can be used directly or indirectly. A direct use of electricity is realized through power-to-heat technologies such as heat pumps and battery electric vehicles can be used in the transport sector. The indirect use is represented by power-to-gas plants. Power-to-gas plants such as electrolyzers and methanation plants convert the electrical energy into hydrogen and methane. In this way, the energy can be stored in the gas grid and used a later time. Power-to-gas technologies offer the possibility to produce green fuels to save GHG emissions in industry, heat, and mobility sectors.

Both the electricity grid's demand for flexibility and the gas grid's feed-in capacity are distributed differently from region to region and vary over time. Both factors have a decisive influence on the allocation of power-to-gas plants. In order to determine an optimal allocation of power-to-gas plants in Germany, the spatially and temporally resolved installable

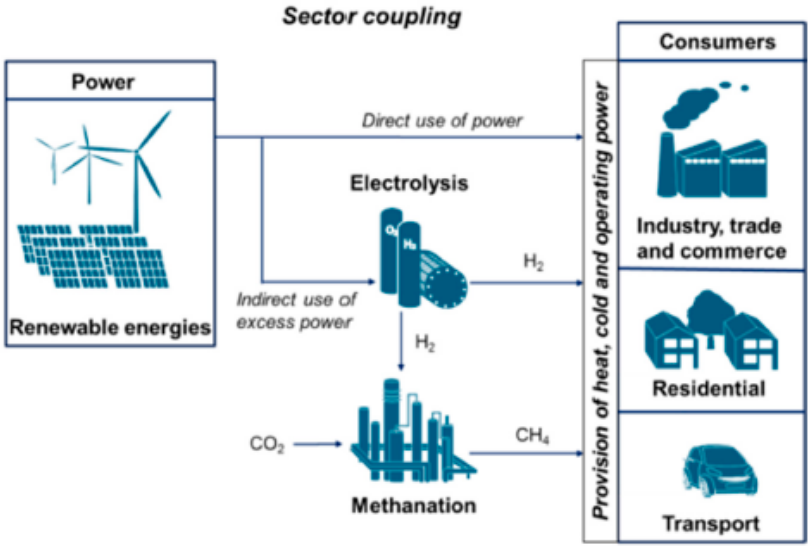

Figure 1.2: The principle of sector coupling [2]

capacity of power-to-gas plants feeding into the gas grid is determined in this work. Using the determined installable capacity of power-to-gas plants, the following research questions are answered:

How does the spatial distribution of the installable capacity of power-to-gas plants influence the allocation of power-to-gas plants?

How does the temporal distribution of the installable capacity of power-to-gas plants influence the allocation of power-to-gas plants?

What is the impact of maximum permitted concentration of hydrogen in the gas grid on the allocation of power-to-gas plants?

2 Fundamentals

2.1 Power-to-gas

The increase of weather-dependent RES requires different flexibility options, under which power-to-gas is a much-discussed option as long-term storage and sector coupling option [8]. PtG links the electricity and the gas grid through conversion of electricity into hydrogen (H_2) or methane (CH_4). Electrolyzers are used to convert electricity in hydrogen. In an additional process called methanization, hydrogen is converted into methane. These products can be utilized directly in industry or fed into the gas grid. In the following subsections electrolysis and methanization are described shortly.

2.2 Water Electrolysis

An electrolyzer is composed of two electrodes, an electrolyte and a diaphragm. An electrical potential between the electrodes is used to split water in hydrogen and oxygen. The chemical reaction of water electrolysis is described by Equation 2.1.

$$H_2O \rightarrow H_2 + \frac{1}{2}O_2 \tag{2.1}$$

Applying a direct current produces hydrogen at the cathode and oxygen at the anode [18]. The electrolyte is capable of conducting ions, which allows an electric flow between the electrodes. The electrodes are separated by an electric isolator in order to avoid a flammable mixture of the product gases. Electrolysis is an endothermic process and its enthalpy of reaction is composed of an electric and a thermal part. Thus, the proportion of electrical energy to be supplied decreases with increasing process temperature. Energy demand for heat has to be considered [19]. There are three main water electrolysis technologies, which can be distinguished by their electrolyte. The three types are alkaline water electrolysis,

proton exchange membrane (PEM) electrolysis, and high-temperature electrolysis. In the following subsections their characteristics are described.

2.2.1 Alkaline water electrolysis

In alkaline water electrolysis potassium hydroxide (KOH) with a concentration of 20 wt.% to 40 wt.% performs as electrolyte [19]. A gas-tight diaphragm allows transport of hydroxide ions (OH^-) and avoids mixture of evolving gases. The porous electrodes are usually made of nickel and mounted directly on the diaphragm [20].

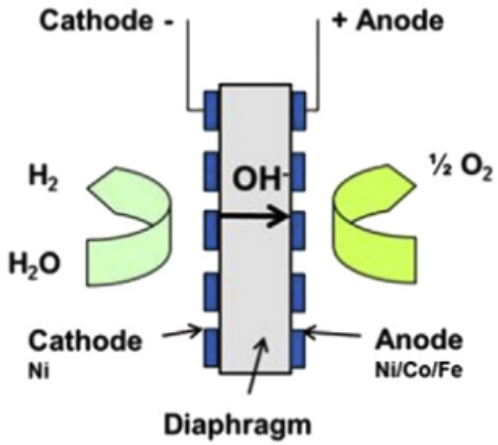

Figure 2.1: Schematic design of an alkaline water electrolyzer [3]

The schematic design of an alkaline water electrolyzer is shown in Figure 2.1. Applying a direct current produces hydrogen at the cathode according to reaction 2.2 and oxygen at the anode according to reaction 2.3 [19].

$$2H_2O(l) + 2e^- \rightarrow H_2(g) + 2OH^- \tag{2.2}$$

$$2OH^- \rightarrow \frac{1}{2}O_2(g) + H_2O(l) + 2e^- \tag{2.3}$$

The operating temperatures of alkaline water electrolysis are in the range of 70 °C to 90 °C and the current densities are in a range of 0.3 A cm^{-2} to 0.5 A cm^{-2} [20]. According to [18] the median of alkaline electrolysis efficiencies in literature is 67 % and in established projects

68 %. The nominal power of the electrolysis is denoted in the following by P_N. Even though alkaline water electrolysis is slower in terms of dynamics than PEM electrolysis, a dynamic load change rate of 10 % P_N/s is fast enough for grid applications. In terms of minimal part-load capability in literature is shown that alkaline water electrolysis is limited to 20 % to 40 % P_N. Thus, using alkaline water electrolysis a stack efficiency of up to 67 % can be achieved. Alkaline water electrolysis modules achieve a capacity of up to 2.5 MW_{el} and operating pressures up to 30 bar.

2.2.2 Proton exchange membrane electrolysis

PEM electrolysis consists of a proton-conducting polymer membrane, which is used as electrolyte and diaphragm. The electrodes are directly connected to the membrane. Figure 2.2 shows the schematic design of a PEM electrolyzer.

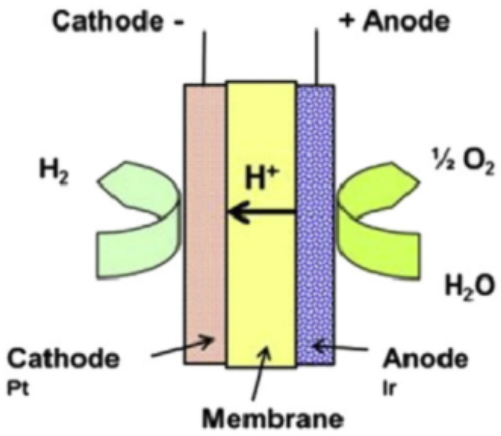

Figure 2.2: Design of a proton exchange membrane electrolyzer [3]

The process of electrolysis is described by the following Equations. The reactions at cathode and anode are defined by Equation 2.4 and Equation 2.5. As in alkaline electrolysis, the hydrogen is produced at the cathode and oxygen is produced at the anode [19].

$$2H^+ + 2e^- \rightarrow H_2 + 2OH^- \tag{2.4}$$

$$H_2O \rightarrow 2H^+ + \frac{1}{2}O_2 + 2e^- \tag{2.5}$$

Proton exchange membrane electrolysis is operated at temperatures around 80 °C [3]. The PEM electrolysis is capable of high current densities of 0.5 A cm^{-2} to 2 A cm^{-2} as well as low part-loads of 0 % to 5 % P_N. While the cell efficiency is similar to that of alkaline electrolysis the stack efficiency is lower. PEM electrolyzers are only available on a small scale and provide hydrogen at pressures up to 100 bar [3].

2.2.3 High-temperature water electrolysis

High-temperature water electrolysis is still at the stage of research. Solid oxide, which consists of yttrium oxide-stabilized zirconium oxide, is used as the electrolyte. The electrolyte conducts O^{2-} ions. The design of a high-temperature water electrolyzer is shown in Figure 2.3.

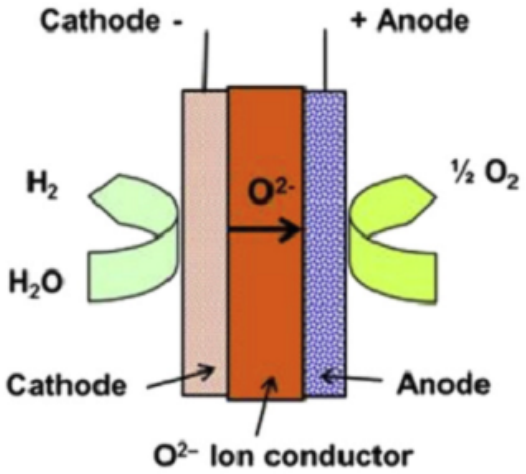

Figure 2.3: Schematic design of a high-temperature electrolyzer [3]

The reaction at the cathode is given by Equation 2.6. The anode reaction is defined by Equation 2.7.

$$H_2O + 2e^- \rightarrow H_2 + O^{2-} \tag{2.6}$$

$$O^{2-} \rightarrow \frac{1}{2}O_2 + 2e^- \tag{2.7}$$

For the electrolysis steam is used instead of water at an operating temperature around

700 °C to 1000 °C. A water-splitting reaction at high temperatures leads to the advantage of high-temperature water electrolysis, the thermodynamic effect. The electric efficiency is defined as the ratio of chemically bound energy output to electric input. Due to the thermodynamic effect a part of the required enthalpy can be provided by high-temperature heat instead of electric energy. Thus the electric efficiency can exceed 100 %.

2.3 Methanation

In an additional process synthetic methane can be produced by methanation. The advantage of methane over hydrogen is the possibility of unrestricted use of the natural gas grid. There are two types of methanation, which are explained in the following subsections.

2.3.1 Chemical Methanation

Chemical methanation is also known as Sabatier process. The process is composed of a water-gas shift reaction and the methanation which are given by Equation 2.8 and Equation 2.9 [19].

$$H_2 + CO_2 \rightarrow CO + H_2O \tag{2.8}$$

$$3H_2 + CO \rightarrow CH_4 + H_2O \tag{2.9}$$

$$4H_2 + CO_2 \rightarrow CH_4 + 2H_2O \tag{2.10}$$

To decrease the needed reaction temperature nickel- and ruthenium-based catalysts are used. The operating temperature of chemical methanation is in the range of 200 °C to 600 °C. The operating temperatures below 200 °C must be avoided to prevent the formation of catalyst poison [19]. The process is operated at pressures of 1 bar to 100 bar [18]. The efficiency of the process is limited to 83 % because 17 % of the chemical energy of hydrogen is released as heat [3]. The process efficiency can be increased by using the heat in the process [19]. The excess heat can be used to supply steam in case of using high-temperature electrolysis, to supply heat for internal processes and to generate power using organic rankine cycle (ORC) process. Another option for excess heat usage is the integration of a heat sink such as district heating network.

2.3.2 Biological Methanation

In biological methanation microorganisms are used. The process is operated at temperatures of 40 °C to 60 °C and pressures of 1 bar to 3 bar [19]. There are two different procedures for biological methanation. Processes with an additional reactor for methanation are called ex-situ. In an in-situ process the methanation takes place in the bioreactor. Using this procedure the yield of the bioreactor should be increased because additional hydrogen is reacting with excess CO_2 [18].

2.3.3 CO_2 sources

Carbon dioxide (CO_2) is required for methanation. Basically, CO_2 sources can be classified by their origin into the categories of green carbon and black carbon. Green carbon comes from climate-neutral sources where the CO_2 cycle is closed and no fossil CO_2 is released to the atmosphere. On the other hand, black carbon releases fossil CO_2. Examples of green carbon sources for CO_2 are atmospheric CO_2 using separation from air via electrodialysis or adsorption, and biogenic CO_2 using separation from biogas. Another source for green carbon is CO_2 recycling, which means the combustion of climate neutral gas and subsequent separation from flue gas and reuse of CO_2. An example for black carbon source is fossil CO_2, which is separated from flue gases of power plants and production sites of cement and steel [19].

3 State of the Art

3.1 Power-to-gas in the energy system

In principle, the possible applications of PtG plants as sector coupling element can be summarized as: using excess electricity from RES, contribution to system stability, supply of green fuels for decarbonizing mobility, heat, and industry sector, and reduction of electricity network expansion through continued use of existing gas network infrastructure [21]. In the gas market, PtG can compensate for declining European gas production and ensure independence from imports [8]. Although PtG is not yet competitive today, it could contribute to stabilizing and decarbonizing the German energy system in the future [22].

3.1.1 Current status of power-to-gas

Currently 153 projects in 22 countries regarding PtG are completed and planned since 1988 [4]. Most of the projects are located in Europe and Germany has the highest share. More than half of all projects focus on hydrogen production. Most electrolyzers used in the projects are PEM electrolyzers and alkaline electrolyzers. Only a small percentage use high-temperature electrolyzers. And looking at methanation half of the projects are using biological methanation and the other half are using chemical methanation process. Figure 3.1 shows the allocation of realized power-to-gas plants in Germany. A distinction is made between the product gases hydrogen, methane, chemical feedstock and liquid organic hydrogen carriers (LOHC). Product gases are injected into the gas grid in 45 % of the projects. The share of feeding in methane is higher than of hydrogen. In 2019 most of the installed PtG plants are located in Germany with a total installed power of 30.7 MW_{el}. Over the past years the average plant size has been rising. The average plant size of methanation is 380 kW_{el} per facility and the average electrical power of an electrolyzer is 430 kW_{el}.The total average plant size of both technologies is 407 kW_{el} and is estimated to increase up to 0.7 MW_{el} by 2050.

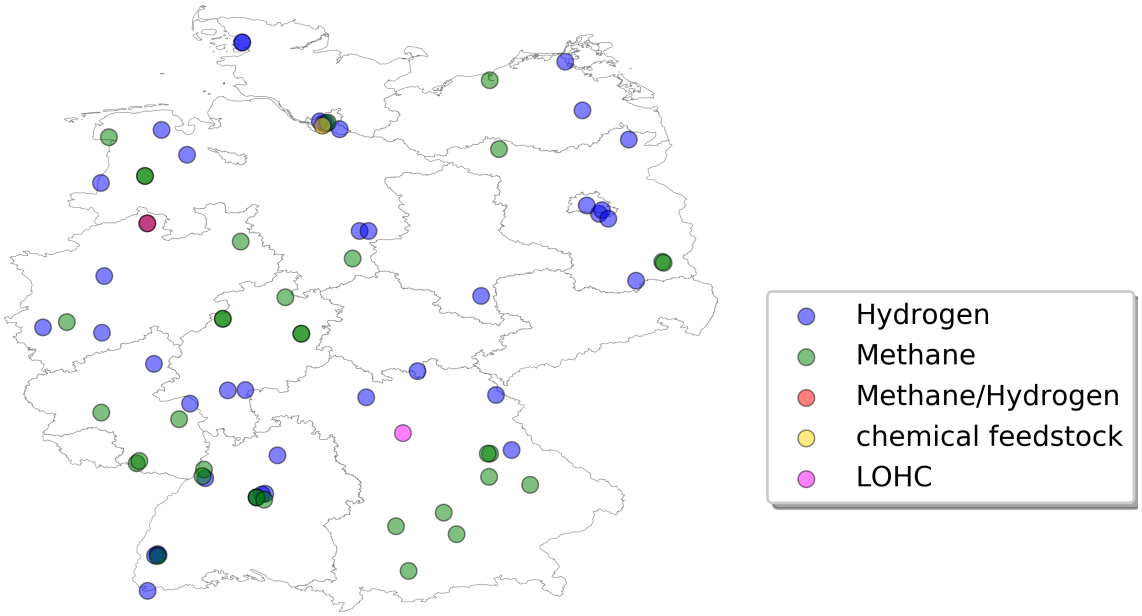

Figure 3.1: Power-to-gas plants in Germany according to Thema et al. [4]

Investment costs of PtG technologies are expected to decrease. Nowadays average costs of alkaline electrolyzers are about 1300 €/kW_{el}. It is estimated that the costs decrease below 500 €/kW_{el} by 2050. The costs for PEM electrolyzers will decrease from 1900 €/kW_{el} to 500 €/kW_{el} by 2050 and the costs for high-temperature electrolysis are expected to fall from 3570 €/kW_{el} in 2017 to 535 €/kW_{el} by 2050 [4]. The cost reduction for chemical and biological methanation is estimated to decrease from 1230 €/kW_{el} to 130 €/kW_{el} to 400 €/kW_{el} for chemical methanation and from 1980 €/kW_{el} to 200 €/kW_{el} to 400 €/kW_{el} for biological methanation by 2050 [23]. Other sources state a decrease of hydrogen electrolyzer costs to 350 €/kW_{el} and the costs of methanation plants to 750 €/kW_{el} by 2030 [24].

3.1.2 Network development plan

The federal government passed the climate protection law in 2019, which set aims for each sector to reduce GHG emissions until 2030. In addition to increasing energy efficiency, the changeover to RES plays a particularly important role. In building, transport and industry sectors, only a few RES are used directly such as solar thermal energy or biogenic fuels. Heat pumps, electromobility or PtG are technologies which indirectly draw on RES through

the use of electricity and can benefit from the high share of RES in electricity sector. Since comparatively emission-free energy can be generated easily and efficiently within the electricity sector, the electricity sector thus plays a key role in decarbonization the other sectors. Despite the measures taken to increase energy efficiency, electricity demand is expected to rise in the future, especially due to the coupling of the electricity sector with other sectors.

The network development plan for gas examines, among other things, the future development of gas demand [5]. Figure 3.2 shows the development of gas demand according to various scenarios up to 2050. The y-axis indicates the change in gas demand in relation to gas demand of the year 2017. Many scenarios show a decrease in gas demand due to increasing efficiency and substitution effects.

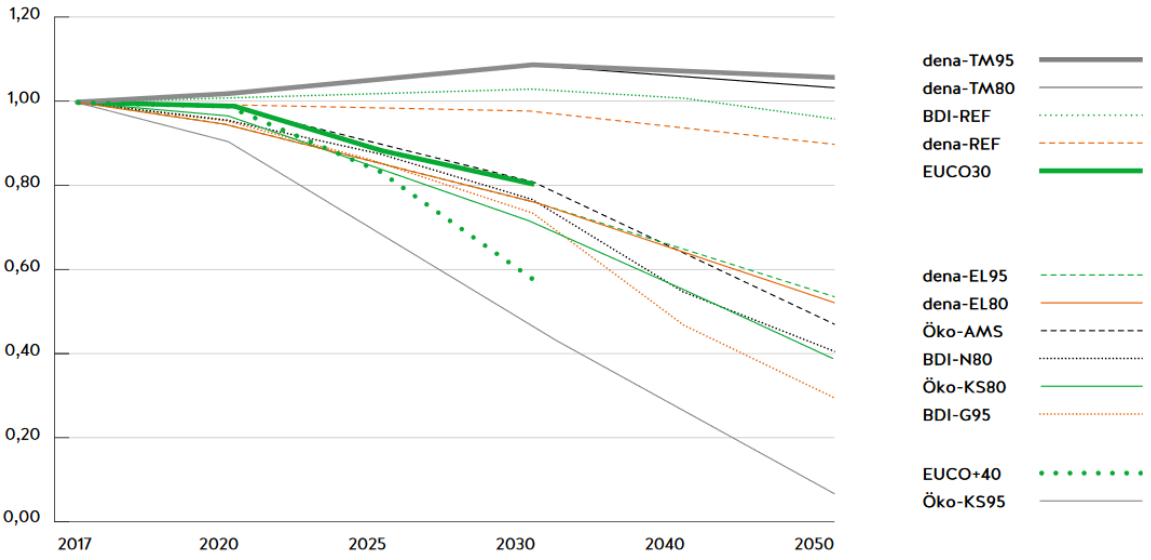

Figure 3.2: Development of gas demand in different scenarios up to the year 2050 [5]

For this work, the EUCO30 scenario is discussed in more detail. In this scenario, it is assumed that the 30 % efficiency target is achieved and that the EU GHG reduction target is met. The gas demand trend for scenario EUCO30 is shown in Table 3.1. A reduction in gas demand can be observed in the industry and household sectors. Despite an increase in gas demand in the transport, non-energetic use of gas and conversion sector, the total gas demand decreases by 20 % till 2030.

The network development plan describes four different scenarios. In the following, scenario C 2035 will be addressed. This scenario assumes the advancing transformation of the elec-

Table 3.1: Development of gas demand in scenario EUCO30 [5]

Gas demand	Unit	2017	2020	2025	2030
Industry	[TW h H_s]	261	261	222	204
Households	[TW h H_s]	394	393	354	313
Transport	[TW h H_s]	2	3	4	8
Non-energetic	[TW h H_s]	38	39	40	40
Conversion sector	[TW h H_s]	274	284	312	329

tricity sector. Sector coupling and the grid-oriented deployment behavior of producers and consumers play a decisive role. Compared with the other scenarios for 2035 of the network development plan, scenario C 2035 has the highest share of gross electricity consumption of RES with approximately 77 $\%$.

PtG plants are differentiated into Power-to-Hydrogen and Power-to-Methane plants. Synthetic methane from Power-to-Methane plants is identical in substance to natural gas and can be integrated into the gas infrastructure. However, the Power-to-Methane process chain includes the additional step of methanation, which reduces the efficiency compared to Power-to-Hydrogen. Therefore, an economical operation is more difficult to achieve than with Power-to-Hydrogen. Hydrogen can be used materially and energetically. High hydrogen demand is expected in industrial sectors such as the chemical industry and steel industry. In the chemical industry hydrogen is used to produce other chemicals, like in ammonia synthesis. In the steel industry hydrogen can replace coke as a reducing agent in the refining of iron, which would be associated with a considerable reduction in GHG emissions. The hydrogen demand in the industry sector is estimated at 78.5 TW h in 2035 [25]. The energetic use of hydrogen offers a high potential for decarbonizing the mobility sector using fuel cells. In order to substitute natural gas, hydrogen can be fed into the gas infrastructure.

The capacities planned for the expansion of PtG plants and the assumed full load hours are shown in Table 3.2. The scenario C 2035 states that a part of the hydrogen supply will be provided by electrolyzers with a total capacity of 4.5 GW, located directly at the industrial sites. In addition, it is assumed that additional electrolyzers will be built, which will operate primarily on a grid-oriented basis. To avoid congestions in the transmission grid, a total capacity of 3 GW is provided using these grid-oriented electrolyzers. The German national hydrogen strategy states that up to 5 GW total electrolyzer capacity will be established by 2030 [26]. In the case of Power-to-Methane, it is assumed that 0.5 GW total capacity of

Power-to-Methane plants will be built by 2035.

Table 3.2: Network Development Plan Scenario C 2035

Power-to-Gas	**PtG capacities** [GW]	**full load hours** [h]
Power-to-Hydrogen at industrial sites	4.5	3500
Power-to-Hydrogen grid-oriented	3	1500
Power-to-Methane	0.5	1000

Most of the plants produce hydrogen for the local demand of industrial sites and due to the high investment cost of electrolyzers, a design of the plants to high full load hours is reasonable. The use of hydrogen storage tanks allows for flexible operation of the electrolyzers. In total, the network development plan states an operation with 3500 full load hours. Electrolyzers used for grid-oriented operation are feeding directly into the natural gas grid. Due to this, there is competition with the costs of conventional gas. These electrolyzers are only used in low electricity prices or congestions in the transmission grid. Therefore, grid-oriented operating electrolyzers are expected to operate at 1500 full load hours. Power-to-Methane plants compete with conventional natural gas supply and therefore are only used at very low electricity prices. This leads to the assumption that power-to-methane plants are operated at 1000 full load hours per year.

As PtG plants represent the link of electricity and gas grid by converting electricity to hydrogen (H_2) or methane (CH_4), they can operate to support the stability of both grids. Many factors influence the potential for PtG plants. One of the influence factors is the gas grid and the possibility to feed-in additional gas produced by PtG plants.

3.2 Gas grid

The distribution of PtG plants is significantly influenced by the capacity of the natural gas grid. The German gas network has a total length of 511 000 km. The pipeline systems enable the distribution, transport and safe delivery of the required quantities of gas over long distances at any time for buildings and households, industry and commerce, and the mobility sector throughout Germany. In addition, large quantities of gas are transported via German territory to other EU countries. In this way, the gas infrastructure contributes significantly

to trans-European networking and to ensuring EU-wide system stability. The network can be divided into a transmission grid using high pressure pipelines and a distribution grid that transports the gas to the end consumer. The transmission grid is distinguished by diameter and pressure into six classes (A-F). The maximum transport capacity of a pipeline results from the assignment of a pipeline to pipeline classes, as shown in Table 3.3.

Table 3.3: Classification of transmission grid pipelines [8]

Class	**Pressure** [bar]	**Diameter** [mm]	**Transport capacity** [GWh_{th}/d]	**Upper boundary** [MW]
A	100	$x \geq 1000$	$1275 - 436$	53125
B	$25 - 100$	$700 \leq x < 1000$	$159 - 399$	16625
C	$25 - 63$	$500 \leq x < 700$	$111 - 179$	7458
D	25	$350 \leq x < 500$	$20 - 54$	2250
E	$16 - 25$	$200 \leq x < 350$	$9 - 22$	917
F	63	$100 \leq x < 200$	6	250

The German gas grid offers a total gas storage potential of 130 TWh_{th} for natural gas [27]. There is an upper limit for the supply of hydrogen into the gas grid, which results from the downstream applications. For the existing natural gas infrastructure a maximum permitted hydrogen concentration of 5 vol.% is assumed [7] [28]. But the raising of the maximum permitted hydrogen concentration in the natural gas grid up to 15 vol.% is discussed [7]. Assuming a volume fraction of 5 % hydrogen, the storage potential for hydrogen in gas grid is about 15 TW h [28]. The influence of a rising maximum permitted hydrogen concentration should also be investigated. The allocation and size of PtG plants may be affected by this restriction. Therefore, a high spatial resolution is required to represent the influence of the restriction.

3.2.1 LKD-EU Data for modelling the gas grid

As part of the LKD-EU research project, a data set of the German electricity, heat, and natural gas sectors was developed. This data set aims to document the status quo of the German energy sector.

The following paragraphs focus on the data related to the gas sector. The data set gives information on the natural gas transmission grid, natural gas demand, natural gas supply, and natural gas storage in Germany. The data on the natural gas transmission grid is

mainly based on the 16 transmission system operators (TSOs) in Germany. Data provided by TSOs differs with respect to quality and extent of technical details. The pipeline system is modeled using the directed graph theory. The pipelines are divided into the six classes of Table 3.3 according to pressure and diameter. The maximum transport capacity of each pipeline class is estimated using the nominal pipeline pressure and diameter and can be interpreted as the upper bound for real-world transport capacities. The total length of modeled pipelines amounts to 32 075 km and is lower than the length of 36 843 km documented by TSOs. Reasons for the deviation of modeled pipelines are neglecting curves of pipelines and parallel pipelines that are modeled as a single pipeline. Figure 3.3 shows the transmission grid using the data of LKD-EU.

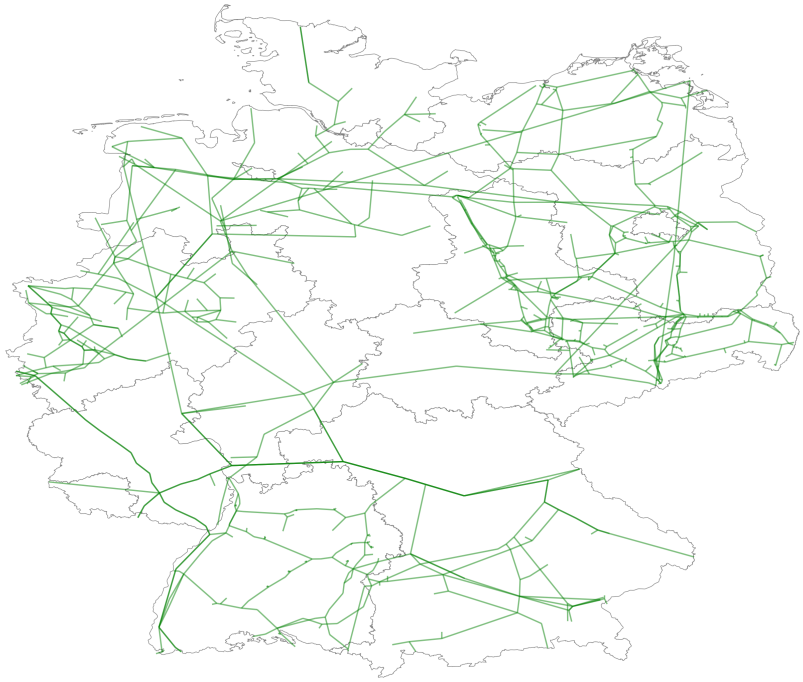

Figure 3.3: Transmission Grid in Germany

Spatial reference units are used to break down geographical data to higher spatial resolution. The NUTS-System (French Nomenclature des unités territoriales statistiques) refers to a hierarchical system for the unique identification and classification of the spatial reference units of official statistics in the European Union member state. While NUTS-1 describes the level of countries, NUTS-2 describes the level of federal states. A NUTS-3 area is characterized by the number of inhabitants in a specific region and is defined by a minimum number of 150 000 inhabitants and an upper bound of 800 000 inhabitants. Table 3.4

provides an exemplary classification of German regions.

Table 3.4: Classification of NUTS-Levels [9]

Region	Name of region	NUTS-Level
Country	Germany	NUTS-0
Federal state	Hessen	NUTS-1
Governmental district	Kassel	NUTS-2
County	Schwalm-Eder-Kreis	NUTS-3

Data on natural gas demand is given in a spatial resolution in NUTS-3 regions. Both a top-down and a bottom-up approach were used to resolve the total natural gas demand. In a top-down approach the specific information is disaggregated from a level with low spatial resolution to a more geographically detailed level using certain rules and methods. This process is also called regionalization. In contrast, a bottom-up approach starts on a level with higher resolution and summing the information of each part to get information of the total geographical area [6]. The natural gas demand can be divided into different sectors. In this data set the gas demand is divided into the sectors industry, heat, and the demand of natural gas power plants. The transport sector is neglected due to low share of natural gas demand. The data is clustered according to regions using the NUTS-3 level. Figure 3.4 shows the natural gas demand of each sector per NUTS-3 region. In the following paragraphs, the sector-specific determination of the spatial resolution at NUTS-3 level is discussed.

The industry sector is divided into eight energy-intensive branches such as chlorine, food, tobacco, glass, ceramics, paper, steel and aluminum. The allocation of the gas demand to NUTS-3 regions follows a top-down approach. The sector-specific gas demand is distributed to NUTS-3 regions according to the number of firms per region. Figure 3.4a shows the gas demand of the industry sector on NUTS-3 level.

The natural gas demand for electricity generation is given for NUTS-3 regions using the location of gas-fired power-plants. The gas demand is shown in Figure 3.4b.

The natural gas demand for heating is also given on NUTS-3 level in this data set. The gas demand of the heat sector is significantly driven by households. The technologies for the provision of heat vary from household to household. In addition, the heat demand and thus also the gas demand depends on the building structure. The spatial resolution is calculated using regional structures of buildings and heat technologies. Figure 3.4c shows the spatially

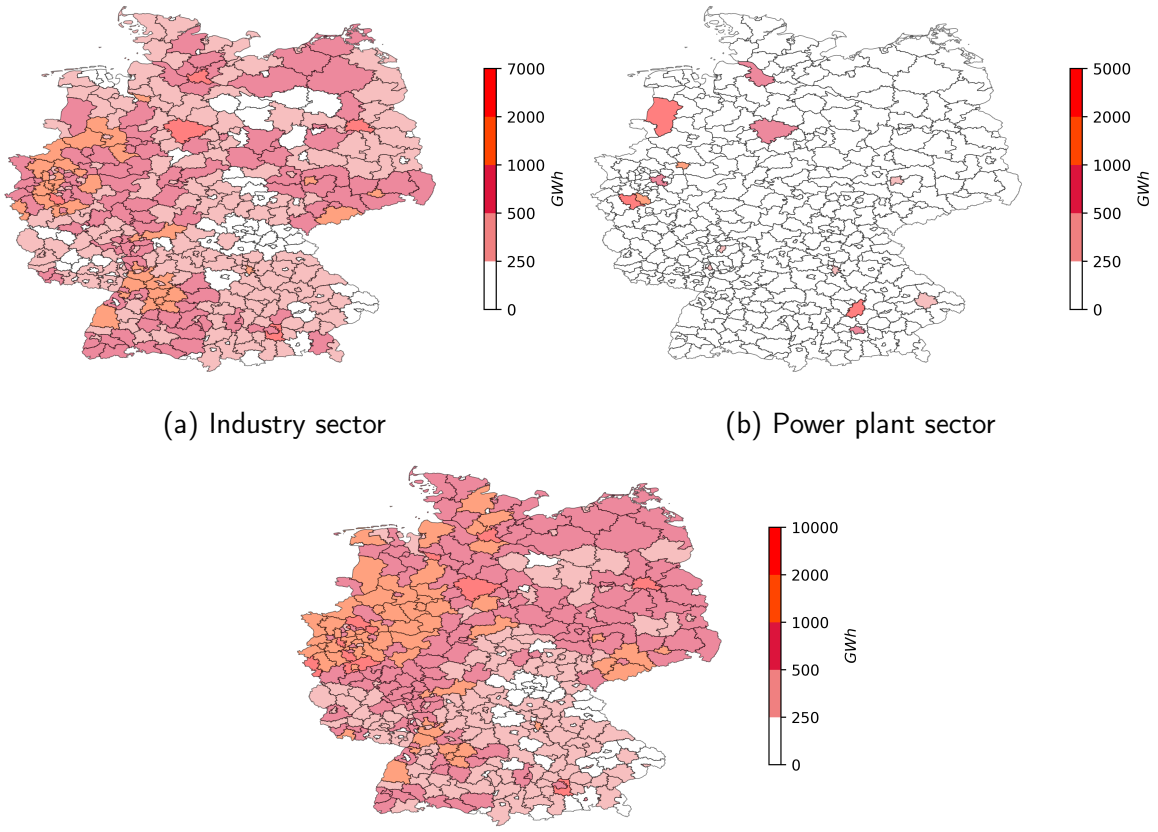

(a) Industry sector

(b) Power plant sector

(c) Household sector

Figure 3.4: Natural gas demand per NUTS-3 region according to LKD-EU data set, own illustration [6]

resolved gas demand of the heating sector. In the LKD-EU study, the determined data on gas demand for heating is compared to public information for all federal states on gas demand for heating. Comparing the data sources shows that the approach overestimates the residential natural gas demand. One reason might be the higher share of buildings that are supplied by district heating [6].

The approach of modeling the gas demand is limited because it requires a range of assumptions and simplifications. First, it focuses on the sectors industry, heat, and electricity, while it neglects transportation. Also, combined heat and power (CHP) plants producing heat and power simultaneously are not considered. Industrial processes that use natural gas both as raw material and as an energy source are neglected. In the heating sector, the focus is on private households, while public buildings are underrepresented. In the industry sector, the allocation of industrial natural gas demand focuses on energy-intensive

industries. Remaining gas demand by industry is distributed using a simplified approach of using gross value added (GVA) as a distribution key. This could lead to distortion in urban areas.

Data on natural gas production in Germany is also given in a spatial resolution on NUTS-3 level. In this data set shale gas exploration is not considered because it is forbidden in Germany and the production costs can not compete with conventional natural gas. Biogas is not taken into account as well because most biogas is used to produce heat and power in CHP plants and only a small number of biogas plants is injecting into the gas grid. Additionally, the share of biogas from the total natural gas demand was only 1.5 % by 2015.

There are limitations of this data set and approaches concerning the natural gas system. Data provided by the TSOs consists of limited details of technical features. Capacities of transmission grid pipelines are calculated based on assumed pressure and diameter information. The transport sector and losses of the gas grid are neglected in the determination of gas demand. For the gas production biogas is not considered in this data set [6].

3.3 Determining potential feed-in capacities of Power-to-Gas into the German gas grid

One of the influence factors of allocating PtG plants is the possibility of feeding-in additional gas produced by PtG plants. One of the main objectives of this work is determining the potential of the German gas grid as storage for gas produced by PtG plants in a high spatial and temporal resolution. The high spatial and temporal resolution enables a precise allocation of PtG plants by taking into account the local conditions of the gas grid. The gas injected by PtG plants into the gas grid substitutes the natural gas. Hence, the potential can be determined in two ways. The potential can be determined by calculating the transport capacity of the pipelines using their dimensions. Likewise, the potential can be determined by calculating the gas demand covered by PtG plants instead of by conventional gas. A top-down or a bottom-up approach can be used to determine the demand.

3.3.1 Literature on regionalization

In this work, six main studies are reviewed and utilized for the development of spatially and temporally resolved feed-in capacities: von Roon et al. [29], Hüttenrauch et al. [7], Estermann et al. [30], Moser et al. [21], Michaelis et al. [31], and Kunz et al. [6]. Table 3.5 provides a summary of the studies on regionalization selected for review.

Von Roon et al. [29] investigate the demand of gas produced by PtG plants. Regionalization factors are derived to identify attractive regions with regard to the respective location factor. The study addresses location factors such as spatial distribution of hydrogen demand, existing PtG plants and biogas plants. In this study, a spatial resolution of NUTS-3 areas is considered. For determination of hydrogen demand the industry and transport sector are taken into account.

In the study of Hüttenrauch et al. [7] the advantages of coupling electricity and gas sector are investigated. The potential for storing and distributing RES by combining electricity and gas grids is determined. This is done by modeling both grids. In this study, the gas demand and the resulting potential for power-to-gas plants are determined on a NUTS-3 level. Regionalization methods are developed for the sectors industry, private households, power plants, and commerce, trade and services. In addition, methods are used for high temporal resolution on an hourly basis. Operating strategies for integrating PtG plants into the energy system are discussed.

Estermann et al. [30] investigate the theoretical potential of power-to-heat and power-to-gas plants in Germany for substituting conventional energy sources. In this study regionalization rules are developed to distribute the resulting potentials on NUTS-3 level. The potential is determined within the framework of various scenarios. To determine the potential of PtG plants the sectors industry, private households, power plants and commerce, trade and services are considered. Operating strategies of PtG plants are derived.

The purpose of Moser et al. [21] is to estimate the installation potential of PtG plants in the German electricity- and gas distribution grid. For this, the feed-in capacity of the gas distribution grid is investigated. In contrast to the studies mentioned above, a bottom-up approach is applied. Thus, the feed-in capacity is determined on spatial resolution of counties, which is a higher resolution than NUTS-3 level, and aggregated to Germany's total capacity. Also, an hourly temporal resolution is used.

Michaelis et al. [31] investigate the limitation factors of integrating PtG plants into the

Table 3.5: Overview of selected studies

Study	**Spatial resolution**	**Temporal resolution**	**Sectors** industry/ private households/ power plants/ commerce trade services/ transport	**Operating strategy**
von Roon et al. [29]	NUTS-3	-	✓/-/-/-/✓	-
Hüttenrauch et al. [7]	NUTS-3	1 h	✓/✓/✓/✓/-	✓
Estermann et al. [30]	NUTS-3	-	✓/✓/✓/✓/-	✓
Moser et al. [21]	Municipality	1 h	-/-/-/-/-	-
Michaelis et al. [31]	-	-	-/-/-/-/-	✓
LKD-EU [6]	NUTS-3	1 h	✓/✓/✓/-/-	-

energy system. For this, economic and regulating factors are discussed. Three operation strategies for PtG plants are explained, which allow integration. Important location conditions for PtG plants that impact economic operation, such as limits for feeding-in hydrogen into the gas grid, are discussed.

The purpose of the LKD-EU study is to compile a data set for describing the electricity, heat and gas sector. Thus, the objective is to document a data set representing the status quo of the German energy sector. The data set is given in a spatial resolution on NUTS-3 level. For determining the natural gas demand the sectors industry, private households and power plants are considered. The spatial resolution is created using regionalization methods for each sector. Additionally, the data is temporally resolved on an hourly basis. In the following subsections the different regionalization methods are discussed in detail.

3.3.2 Regionalization

In order to determine the feed-in potential of the German gas infrastructure, transmission and distribution grids need to be considered separately. The gas demand in high spatial resolution is used to determine feed-in capacity of the distribution grid. The underlying assumption here is that, due to the low storage capacity of the distribution grids, green fuels can only be injected in the amount of the gas demand [7]. Basis for determining the potential of PtG plants injection into the gas grid is the regionalization of gas demand. Regionalization is the distribution of information from a geographic unit with low spatial resolution to one with high spatial resolution, as shown in Figure 3.5

For the gas demand in distribution grids are the relevant sectors households, commerce, trade and services, industry and transport. The gas-fired power plants in the transformation sector are in most cases connected to the transmission grid [7]. The starting point is gas consumption in Germany given by sectors. For the determination of feed-in capacities of gas produced by PtG plants, the natural gas demand in high spatial resolution is needed. The reviewed studies use different methods to generate natural gas demand data in different spatial resolutions. Additionally, these studies focus on different sectors. Regionalization methods for the sectors industry, private households, power plants, transport and commerce, trade and services are considered. The following subsection discusses methods for regionalizing the various sectors.

Figure 3.5: Regionalization of information to a higher level of spatial resolution [7]

Regionalization of feed-in capacities in the industry sector

For a regionalization of the industry sector, it is first divided into subsectors according to economic activity. In this way, a distinction between energy-intensive industries such as the chemical industry and non-energy-intensive industries such as the food industry is possible [7]. Also a classification according to the use of hydrogen in the industry is useful. A distinction between the non-energetic and the energetic use of hydrogen makes sense here. Non-energetic use describes the use as a raw material for the production of goods and products and energetic use describes the usage as an energy supplier. Four areas of application for the non-energetic use of hydrogen are distinguished [29]: refineries, methanol production, ammonia production and other. Regionalization of non-energetic hydrogen consumption at NUTS-3 level is achieved by assigning each county a percentage that corresponds to the share of hydrogen consumption in the region [29]. In this way, 100 % of Germany's previously recorded material hydrogen consumption is distributed to counties. In von Roon's study [29], the proportions are drawn up with the aid of the European hydrogen atlas. The industrial energetic hydrogen consumption can be distinguished into 14 economic subsectors. The decisive factor for the subdivision is the classification according to NACE WZ 2008 [32]. As a distribution key for regionalization to the higher spatial resolution the number of compulsory social security employees per economic sector is recommended by [7], [29] and [30]. In addition, energy intensity is taken into account by [29] to reduce

inaccuracy due to administrative industry sites with high employment figures. The study of Hüttenrauch et al. [7] additionally focus on the locations of different energy-intensive industrial sites by performing a manual survey.

Regionalization of feed-in capacities in transport sector

Hydrogen demand in transport sector can be divided into demand of different vehicles such as passenger cars, light commercial vehicles, trucks, rail transport, air transport and inland shipping. In the study by von Roon [29], different methods for regionalization are elaborated. For regionalization of the subsector passenger cars the number of registrations is used. In the case of light commercial vehicles the population density is taken into account and the subsector trucks is spatially resolved using traffic counts. Rail transport and air transport are regionalized using non-electrified rail lines and locations of airports. Inland shipping can be spatially resolved by locations of inland ports. Other studies state that the estimation of the development of hydrogen mobility is subject to comparatively high uncertainties. Hydrogen mobility is depending on further development of battery electric vehicles as they are competing technologies [30]. In the study of Estermann et al. [30], transport sector is neglected due to the uncertainties that make reliable statements difficult. Nevertheless, it is recommended to closely monitor the development of hydrogen mobility because political decisions or technological advances can act as drivers and increase the hydrogen demand on a relevant scale [30]. In determination of the regionalized natural gas demand the transport sector is not taken into account by Hüttenrauch et al. [7] due to low influence on hourly demand.

Regionalization of feed-in capacities in household sector

The natural gas demand of the household sector is decisively influenced by the supply of space heating and preparation of hot water [30]. While preparation of hot water is used throughout the year, space heating is only required when the outdoor temperature falls below a building-specific level. Thus, space heating is affected by outdoor temperature, structure, age and type of the building and the heating technology. Hence, a distribution key for the private household sector results from the parameters number of building types, number of apartments, population, hot water consumption, heating technology and climate factor [7].

Regionalization of feed-in capacities in power plants sector

The natural gas demand of the electricity sector can be spatially resolved using the locations of natural gas power plants. In the study of Estermann et al. [30] regionalization is carried out on the basis of the consumption of power plants. Additionally, the composition of the power plant fleet can be taken into account [7].

Regionalization of feed-in capacities in commerce, trade and services

Gas demand in the sector commerce, trade and services is mainly used for space heating. Thus, decisive parameters are the area, structure, age and type of building [7]. A subdivision of the sector into more detailed economic sectors allows a more accurate representation of the natural gas demand based on employees per economic sector [7], [30]. In the study of Hüttenrauch et al. [7], the regional highly resolved gas demand for commerce trade and services sector results from a distribution key consisting of the parameters building area, structure, age and type of building and employees per economic sector.

3.3.3 Temporal resolution

In order to design precisely dimensioned PtG plants, the temporal variation of the gas demand must be taken into account. The determination of year-round available feed-in capacities of the gas grid is necessary to increase the number of full load hours of the PtG plants and enable the long-term planning of the plant deployment. These capacities of the natural gas grid can relieve the electricity grids [7]. Spatially and temporally resolved gas demand of the sectors industry, private households and commerce, trade and services can be achieved using sector-specific load profiles and regionally resolved hourly temperature data [7]. The assumption can be made that the load profiles of a sector do not differ regionally [7]. When considering the industry sector each economic sector can be temporally resolved using a sector-specific load profile. This takes into account consumption fluctuations over the course of the day as well as weekday factors. The regional hourly gas demand of the residential sector is mainly due to space heating and thus depends on the outdoor temperature [7]. Space heating is provided when the temperature falls below the building-specific limit temperature. According to Hüttenrauch et al. [7] a distribution key to generate a temporally resolved gas demand in the residential sector takes into account

temperature data and regional characteristics of the building structure. For the determination of the future gas demands in the residential sector, the simplified assumption can be made that the temperature profile is comparable to today. Thus, the temperature-related gas demand behaves similarly [7].

3.4 Determination of Power-to-Gas plants capacity

The feed-in capacities for each sector determined in the previous subsection are summed to obtain the total feed-in capacity into the German gas grid. In the study of Estermann et. al [30] it is assumed that no additional storage facilities are integrated and the gas produced in each geographical unit is consumed locally. A similar assumption is made by Hüttenrauch et al. [7]. Thus, the natural gas production is subtracted from the natural gas demand of the region. The residual load obtained represents the potential for the integration of gas produced by PtG plants [7], as shown in Figure 3.6.

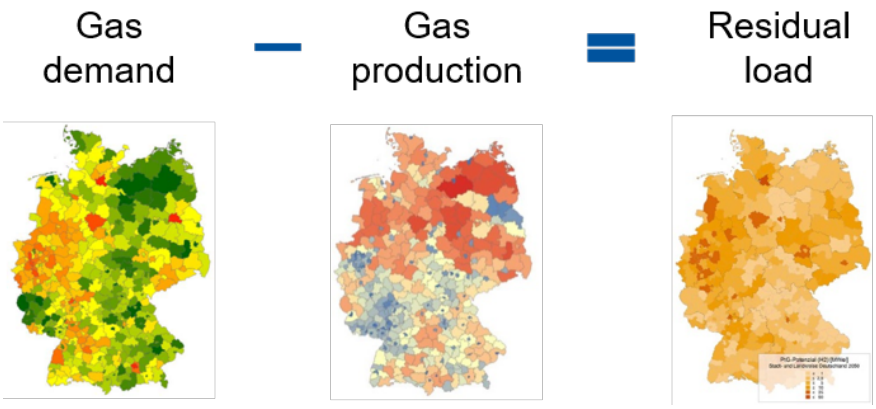

Figure 3.6: Determination of distribution grid feed-in capacity according to Hüttenrauch et al. [7]

While capacities for feeding-in methane into the gas grid correspond to the residual load gas demand, the admixture of hydrogen is limited to a maximum permissible hydrogen concentration. The limit for the admixture of hydrogen depends on the components connected to the natural gas grid. Due to combustion characteristics, an admixture of up to 10 vol.% is considered uncritical [30]. For many components in the gas infrastructure hydrogen concentrations of 10 vol.% are harmless, whereas natural gas tanks in vehicles must not exceed 2 vol.% [16]. A maximum hydrogen concentration of 5 vol.% is assumed for the gas grid

in Hüttenrauch et al. [7]. Consideration of the maximum hydrogen concentration provides feed-in capacity of hydrogen into the German gas grid.

The regionalized feed-in capacities for hydrogen and methane can be used to determine the installable capacity of PtG plants. Here, the feed-in capacities describe the output power of the PtG plants in terms of the thermal energy value of the produced gas. For recalculating the electrical load the efficiencies are taken into account [30], [7].

In the study of Estermann et al. [30] the minimum gas demand is used to determine the capacity of the PtG plants. A design of the PtG plants for the hourly value of the maximum gas demand leads to the fact that the plants run exclusively in partial load operation over the course of the year [7]. Since the feed-in capacities are determined based on the gas demand, the summer nights represent a limiting factor. Here, the minimum gas flow is reached due to the low heating demand. For this purpose, it is suggested to evaluate the time series of the feed-in capacity with regard to the minimum daily mean value and derive the capacity of the PtG plant from it [7].

A different approach to determine the capacities of PtG plants is carried out by Moser et al. [21]. First, the feed-in capacities into the German distribution grids for hydrogen and methane are investigated using a bottom-up approach. The capacities of nine gas distribution grids ranging from villages and small towns to large cities are determined and assigned to specific categories from clusters. The available capacity of the gas grid to feed-in hydrogen or methane from PtG plants is limited by the minimum load occurring in the off-peak hour [21]. As in the other studies described, the feed-in capacity for methane corresponds to the available capacity of the gas grid. Maximum hydrogen concentrations of 2 vol.%, 10 vol.% and 15 vol.% are assumed to determine the feed-in capacity for hydrogen [21].

Estermann et al. [30] propose an expansion of PtG plant capacity from 1 GW to 3 GW by 2035. An expansion in the range of 3 GW to 10 GW by 2050 is conceivable to cover non-energetic hydrogen demand in industry. To cover the entire demand for green fuel in Germany, higher capacities of PtG plants must be installed. According to [33] a capacity of 254 GW must be installed, but for cost reasons not necessarily in Germany.

3.5 Operating strategy

A distinction can be made between three basic modes of operation: market-driven, grid-driven and generation-driven operation [31]. The market-driven operation describes the operation at low prices on the electricity exchange, which is in case of low electricity demand and a high supply by RES. This model of operations requires a short connection to both the electricity and gas grids, as the operation is not controlled by local signals but by central signals from the electricity exchange. The grid-driven operation is used to mitigate congestion situations in the electricity grid. In order to successfully avoid congestion situations in the electricity grid, it is important that the PtG plants are built at the appropriate points in the grid that are affected by overloads. To compensate for fluctuations in power generation of RES and inaccuracies in the forecast of those a generation-driven operation can be used. This operation strategy is carried out in order to optimize the schedule of the power plant fleet of the energy supplier. The same requirements are placed on the site of a generation-driven PtG plant as on a grid-driven PtG plant.

All modes of operation have in common that they are uneconomical today [31]. Estermann et al. [30] state that the operation strategy of the PtG plant depends on the location of its deployment. Thus it is likely that electrolyzers at industrial sites for hydrogen supply will operate at about 7000 full load hours. For the operation of methanation plants feeding into the gas grid, it is recommended to align the operation with the prices of the electricity exchange. A comparison with the price of conventional gas should decide on the use of the plant [30].

4 Methodology

This section provides a detailed description of the methods used in this thesis. First, the methods for the determination of PtG feed-in capacities are explained. The code is implemented as a python tool. In the following section, the energy system model eTraGo is described, which is used to model the electricity grid. Lastly, the procedure for integrating the feed-in capacities into the electricity grid model eTraGo is explained.

4.1 Scenario

The aim of this work is to optimize the allocation of PtG plants in Germany according to the feed-in capacity of the gas grid. In order to be able to make a statement regarding the future development of PtG plants, a scenario from the network development plan is used. In this thesis the scenario C 2035 is assumed which is explained in detail in section 3.1.2. In this scenario, three types of PtG plants are assumed to be built. These are power-to-hydrogen plants feeding into the gas grid, power-to-hydrogen plants covering the hydrogen demand of industrial sites, and power-to-methane plants that directly feed into the gas grid. Therefore, the feed-in capacity of the gas grid for hydrogen and methane must be determined. In order to comply with the scenario, the feed-in capacities must be adjusted to the year 2035. The adjustments of the feed-in capacities to the scenario are explained in the corresponding sections. It is assumed that the absolute level of gas demand changes, but not the regional distribution [7].

4.2 Determination of Power-to-Gas feed-in capacities into the German gas grid

The reviewed studies provide feed-in capacities only at a spatial resolution at NUTS-3 level. Studies at a higher spatial resolution represent a gap in the investigation of feed-in

capacities. To examine the influence of the gas grid characteristics on the allocation of PtG plants, a higher spatial resolution on substation level is needed, as further described in subsection 4.2.1. In addition, limitations such as maximum hydrogen concentration must be taken into account. The determination of the feed-in capacities into the German gas grid is based on the reviewed studies. The methods are being further developed and adapted for a higher resolution. Figure 4.1 summarizes the general procedure of determining the feed-in capacity of the German gas grid.

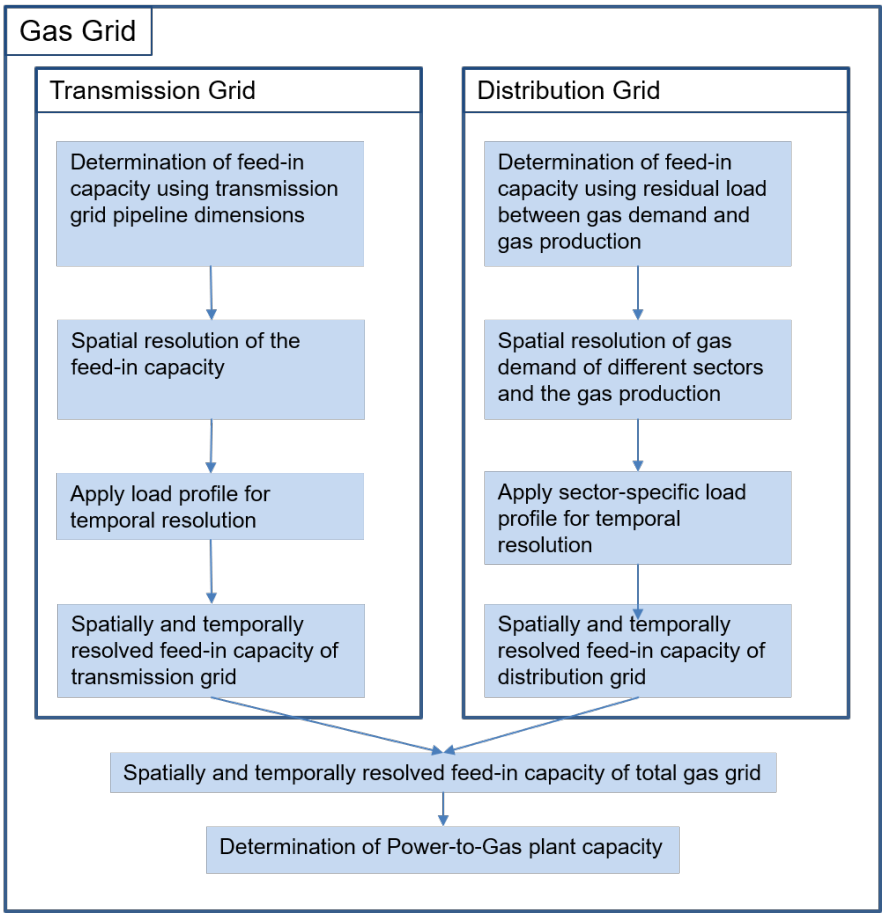

Figure 4.1: General procedure of determining the feed-in capacit of the German gas grid

The gas grid is divided into transmission grid and distribution grid. The potential of feeding-in additional gas produced by PtG plants into the transmission grid is determined via the pipeline dimensions. The feed-in capacity of the distribution grid is obtained in a top-down approach. For this purpose, the natural gas demand is given at NUTS-3 level and is regionalized to a level with a higher spatial resolution. Also the natural gas production is regionalized to the same spatial resolution. It is assumed that the natural

gas produced is consumed locally. Therefore, a residual load is calculated from gas demand and gas production by subtracting gas production from gas demand. The residual load is considered as a potential for feeding-in gas from PtG plants. Subsection 4.2.1 addresses the determination of the spatial resolution of the gas grid in detail.

Subsequently, a temporal resolution of the spatially resolved feed-in capacities is carried out. For this, different load profiles are used, which provide an hourly resolution, as further described in subsection 4.2.2. The feed-in capacities of the total gas grid is obtained by summing up the feed-in capacities for the gas transmission grid and the gas distribution grid. These feed-in capacities represent the output power of the PtG plants in terms of the thermal energy value of the produced gas. The capacity of the PtG plants is determined from the feed-in capacity of the gas grid, as described in subsection 4.2.4.

The methods to obtain the spatially and temporally resolved feed-in capacities are described in detail in the following subsections.

4.2.1 Spatial resolution

In this work, it is assumed that due to scale effects future PtG plants will have an installed capacity in the MW range and are directly connected to the high voltage (HV) power grid. To avoid costs for grid expansion, a short distance between HV substations and the feed-in points of the PtG plants into the gas grid is beneficial.

The energy system model eTraGo provides a data set of so called MV Grid Districts representing the catchment area around the HV-MV substations. The role of these substations in relation to the power grid is described in more detail in section 4.3. By determining the feed-in capacities for these areas, the requirement of short distances between the power grid and the gas grid is taken into account. The data set from the LKD-EU study is used as source data. The data is well suited for the investigation because it contains information on both the dimensions and geographical locations of the gas transmission grid pipelines and the gas demand resolved on the NUTS-3 level. In the following, the feed-in capacities of the gas grid are determined separately for the gas transmission grid and the gas distribution grid.

4.2.1.1 Transmission grid

To determine the feed-in capacity of the gas transmission grid in a high spatial resolution the data set of the MV Grid District and the pipeline data set of the LKD-EU study is used. The topology of the gas transmission grid is superposed with the geometries of the MV Grid Districts. This way, it is checked which MV Grid Districts the gas transmission pipelines pass through. From now on, only the districts that have pipelines will be considered. Each pipeline is assigned a specific class based on its diameter and pressure. The transport capacity of each pipeline class determined by Haumeier et al. [8] is shown in Table 3.3. The feed-in capacity is obtained using the class of the pipeline. The feed-in capacity of the pipeline is allocated to the corresponding MV Grid District. If several pipelines run through an MV Grid District, the capacities are summed up. Figure 4.2 shows the procedure of determining the feed-in capacity of the transmission grid.

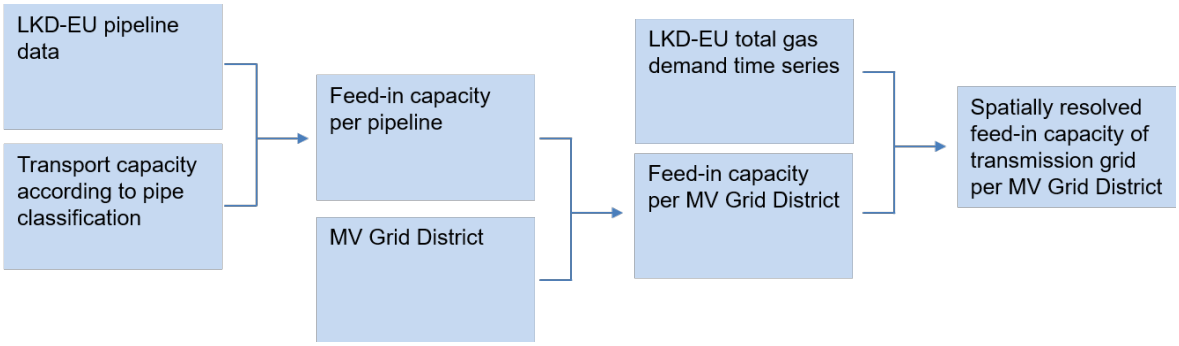

Figure 4.2: Transmission grid procedure

4.2.1.2 Distribution grid

Several assumptions are made to determine the feed-in capacity of the gas distribution grid. It is assumed that the natural gas produced is consumed locally. The residual load can be supplied by PtG plants. Therefore, the gas production is subtracted from the gas demand. In order to determine both gas demand and gas production at the level of the MV Grid Districts, different methods are used. The gas demand is broken down by sector. To quantify the gas demand, the sectors of private households, industry and power plants are considered. Due to the low gas demand, the transport sector is neglected. Additionally, the gas demand is adjusted to the year 2035. The data from the LKD-EU study are applied as input data. These indicate the gas demand broken down by the sectors households,

industry and power plants at NUTS-3 level. The methods used to regionalize these data to the MV Grid Districts are described in the following subsections. Table 4.1 gives a brief overview of the methods used for each sector.

Table 4.1: Methods for the regionalization of the gas demand from NUTS-3 to the level of MV Grid Districts

Household	Industry	Power plant
population	locations of energy-intensive industries	locations of gas-fired power plants

Household sector

The demand of the sector private households is given at the level of NUTS-3. The gas demand of the household sector is mainly influenced by the generation of space heating. Hence, the demand is regionalized using the number of inhabitants. NUTS-3 areas represent the counties in Germany and each county consists of several municipalities. Therefore, the number of inhabitants of the municipalities is used to calculate the gas demand among the municipalities. Overlaps between the areas of the municipalities and the MV Grid Districts are detected. The proportion of the municipality that overlaps with the MV Grid District is determined. This proportion is used to further regionalize the gas demand. The MV Grid District is assigned the proportion of the gas demand of the municipality. In this way, the gas demand of the household sector is regionalized to the level of the MV Grid Districts. Figure 4.3 shows the procedure of determining the spatially resolved gas demand of the household sector.

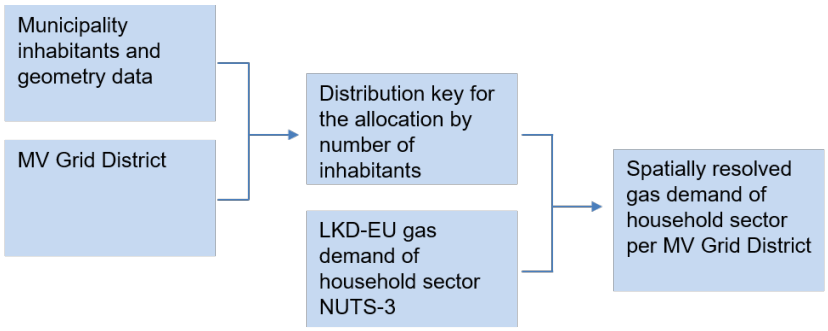

Figure 4.3: Distribution grid household procedure

Industry sector

The LKD-EU study provides gas demand data of the industry sector at NUTS-3 level. In addition, the data set provides locations of energy-intensive industries. It is identified how many energy-intensive industrial sites exist per NUTS-3 area. The gas demand of the industry sector at NUTS-3 level is divided equally among these industrial sites. It is checked in which MV Grid Districts the industrial sites are located and the gas demand is assigned to these districts. If a district contains several industrial sites, their gas demand is summed up. This results in the allocation of the gas demand to the MV Grid Districts. While Figure 4.4a shows the locations of energy intensive industrial sites at the level of NUTS-3, Figure 4.4b shows the same industrial site at the level of MV Grid Districts. The procedure of determining the spatially resolved gas demand of the industry sector at the level of MV Grid Districts is shown in Figure 4.5.

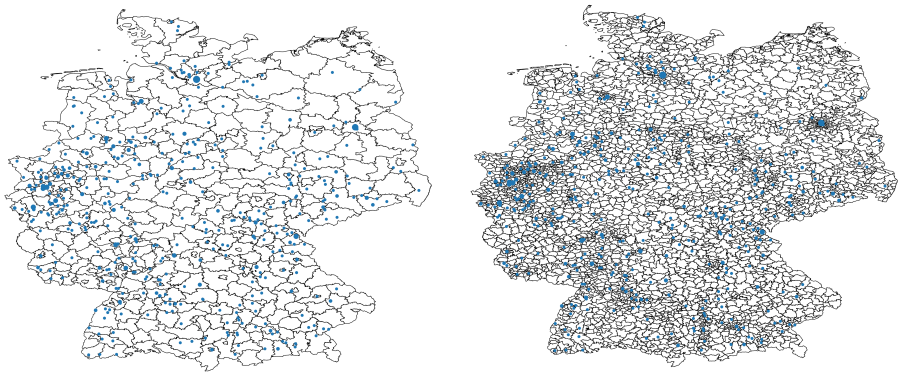

(a) NUTS-3 (b) MV Grid Districts

Figure 4.4: Locations of energy-intensive industrial sites in Germany at the level of NUTS-3 and MV Grid Districts

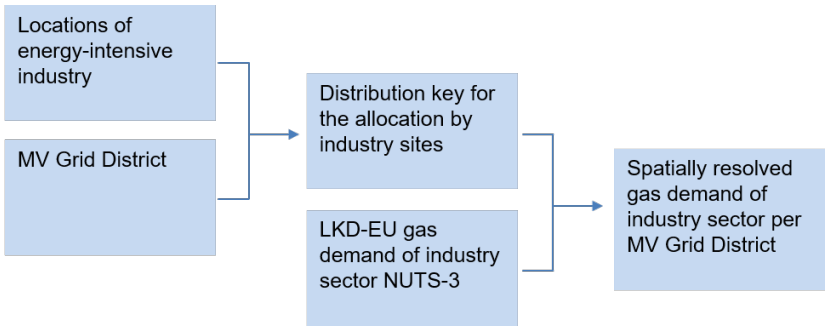

Figure 4.5: Distribution grid industry procedure

Power plant sector

The natural gas demand of the power plant sector is given at the level of NUTS-3 in the LKD-EU study. In order to obtain the gas demand at the level of MV Grid Districts, methods of regionalization are applied. For this purpose, a data set from the federal environment agency on gas-fired power plants is used. These data contain information on the output and location of the power plants. For the regionalization of the gas demand, it is checked which power plants are located in a NUTS-3 area. While Figure 4.6a shows the locations of gas-fired power plants at the level of NUTS-3, Figure 4.6b shows the location of the same gas-fired power plants at the level of MV Grid Districts. The gas demand is allocated to the power plants based on the power plants' output. It is determined how many power plants are located in each MV Grid District. If there are several power plants in a MV Grid District, the gas demand is summed up.

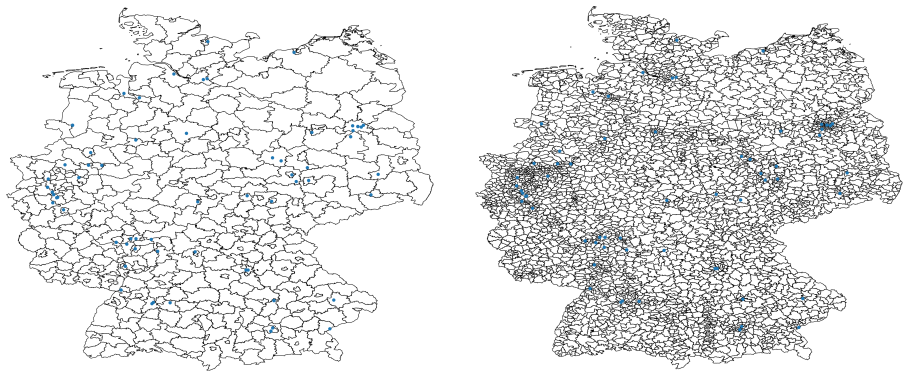

(a) NUTS-3 (b) MV Grid Districts

Figure 4.6: Locations of gas-fired power plants in Germany at the level of NUTS-3 and MV Grid Districts

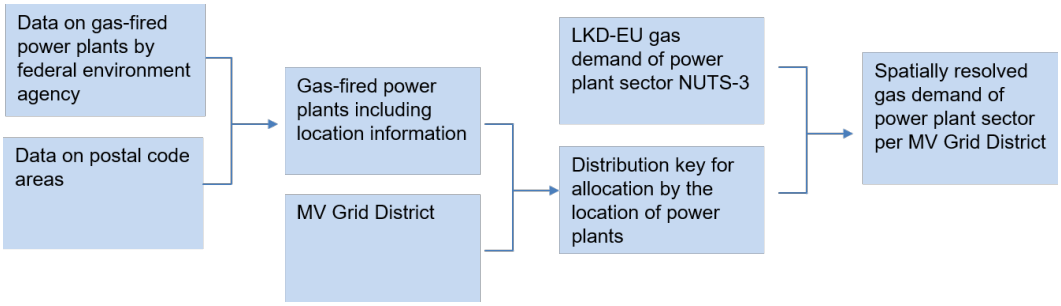

Figure 4.7: Distribution grid power plant procedure

Gas production

The LKD-EU study provides a data on gas production in Germany at the level of NUTS-3. In addition, the locations of gas production sites are given in the study. In order to regionalize gas production to the level of the MV Grid Districts, these sites are used. It is checked which production sites are located in a NUTS-3 area. The gas production of the NUTS-3 areas is allocated to the gas production sites in that area. It is determined in which MV Grid Districts the identified production sites are located. Figure 4.8 shows the procedure of determining the spatially resolved gas production at the level of MV Grid Districts.

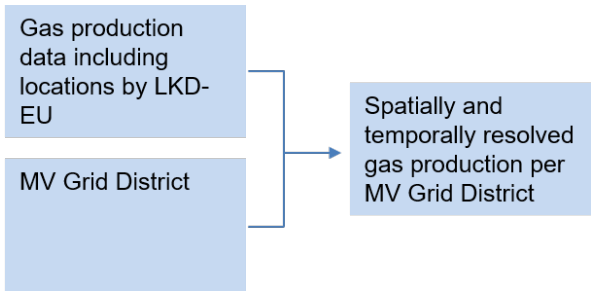

Figure 4.8: Distribution grid production procedure

4.2.2 Temporal resolution

The temporal resolution plays a decisive role in the representation of load peaks. The temporal resolution of feed-in capacities is carried out using sector-specific load profiles. Influencing factors on the temporal distribution such as low gas demand in summer and the production behavior of industry can be taken into account in this way.

4.2.2.1 Transmission grid

The temporal resolution of the feed-in capacity of the transmission grid is performed using a load profile. The assumption is made that the feed-in capacity is dependent on the temperature-related gas demand. The demandlib library[1] is a python tool to create load profiles for electricity and heat on the basis of annual demand data. Using the python tool demandlib a normalized time series for Germany is created. A gas demand time series is

[1] https://github.com/oemof/demandlib

calculated for each NUTS-3 area. The hourly temperature profile of each NUTS-3 area is included in the calculation. In order to obtain an average profile for all of Germany, the mean value of all NUTS-3 areas is calculated for each hour of the year. In the last step the time series is normalized to the maximum value. Thus, a hourly load profile is obtained which can be used to temporally resolve the feed-in capacity of the transmission grid.

4.2.2.2 Distribution grid

Sector-specific load profiles are used for a reasonable temporal resolution of the feed-in capacity into the gas distribution grid. In the following, normalized time series are developed for the individual sectors in order to resolve the feed-in capacities over time. The special aspects of the sectors are addressed.

Household sector

The gas demand of the household sector is significantly influenced by the supply of space heating. Therefore, this dependency also exists for the feed-in capacity into this sector. Space heating is not needed all year and the energy demand for providing space heating is dependent on the structure, age and type of building. When the outdoor temperature drops below a building-specific outdoor temperature, space heating is required. Using the python tool demandlib, an hourly resolved normalized time series is created. In this process, the hourly resolved outdoor temperature over the course of the year is included for each NUTS-3 area. In addition, the general building type is specified. On this basis, the gas demand per NUTS-3 area is resolved over time using a temperature profile. This results in a temporally resolved gas demand at the NUTS-3 level.

Industry sector

The gas demand in the industrial sector is not constant but depends, among other things, on working hours of the industry. Therefore, a normalized time series is applied to resolve the gas demand over time. A few assumptions are made to determine the time-resolved gas demand of the industry sector. It is assumed that the gas demand of the sector industry follows its heat demand. A python tool developed by Schmidt et al. [34] to determine the temporal distribution of the process heat demand is used to obtain a normalized time series.

The tool is taking into account the economic sectors metal, chemical, mineral, mining, food, textile, paper, transport, machinery, and wood industry to identify the process heat demand at the level of NUTS-3 areas. For each economic sector specific load profiles and full load hours are used to generate a temporally resolved process heat demand of each sector. The sector-specific load profiles take into account the different characteristics of production in the respective sectors. This results in a dataset that indicates the process heat demand of the industry sector at NUTS-3 level. The time series of each NUTS-3 area is normalized to its maximum value which provides a load profile for each NUTS-3 area. The load profiles enable an application to the gas demand and a temporally resolved gas demand is obtained.

Power plant sector

The gas demand of the power plants sector depends on the use of gas-fired power plants. Therefore, a load profile of the gas-fired power plants is used to generate the time-resolved gas demand. Data from the federal network agency[2] is used to create the load profile. The data represent a time series of realized electricity generation by gas-fired power plants. The realized electricity generation of the gas-fired power plants is used for the load profile. A mean daily profile is formed from all 365 days of the year. It is assumed that the power plants are operated every day of the year as on the mean day. Thus, the load profile for the entire year is created from the mean daily profile. The load profile is normalized to the maximum value.

4.2.3 Feed-in capacities of the entire gas grid

The determined feed-in capacities of transmission grid and distribution grid apply to the injection of methane into the gas grid. The feed-in capacity of the total gas grid is obtained by summing up the feed-in capacities of the gas transmission grid and the gas distribution grid per MV Grid District. The feed-in capacity of the entire gas grid is determined by:

$$\dot{Q}_{th} = \dot{Q}_{th,trans} + \dot{Q}_{th,dist} \tag{4.1}$$

[2] https://www.smard.de/home/downloadcenter/download-marktdaten

where $\dot{Q}_{th}$ is the feed-in capacity of the entire gas grid for injecting methane into the gas grid, $\dot{Q}_{th,trans}$ is the feed-in capacity of the transmission grid and $\dot{Q}_{th,dist}$ is the feed-in capacity of the distribution grid.

4.2.4 Determination of Power-to-Gas plant capacity

The determined feed-in capacities represent the output power $\dot{Q}_{th}$ of the PtG plants in terms of the thermal energy value of the produced gas. In order to obtain the electrical power of PtG plants, the efficiencies of electrolyzers and methanation plants are taken into account. Figure 4.9 shows the procedure of determining the PtG plant capacity for injecting methane into the gas grid.

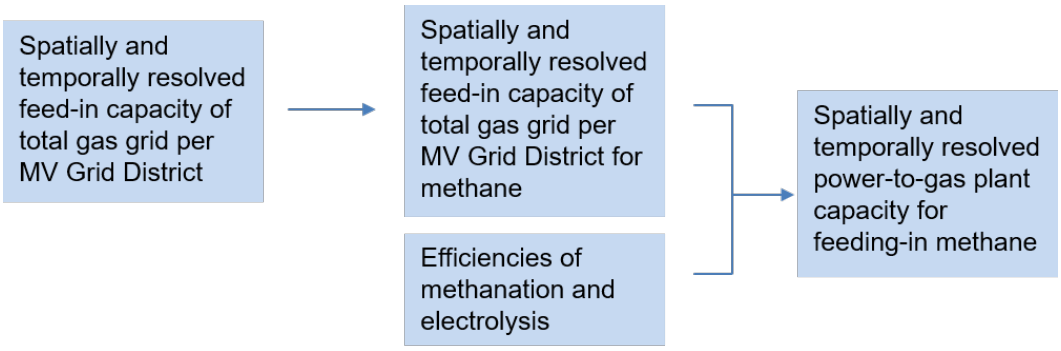

Figure 4.9: Power-to-gas plant capacity for methane procedure

For the transformation of electrical power to the thermal power of methane electrolyzers and methanation plants are used. The electrical power of these plants is calculated using their efficiencies as shown by Equation 4.2:

$$P_{el,methanation} = \frac{\dot{Q}_{th}}{\eta_{methanation} \cdot \eta_{electolyzer}} \tag{4.2}$$

where $P_{el,methanation}$ is the electrical power that can be stored in the gas grid, $\eta_{methanation}$ represents the efficiency of the methanation plant, $\eta_{electrolyzer}$ is the efficiency of the electrolyzer and $\dot{Q}_{th}$ stands for the feed-in capacity of the gas grid for methane, as calculated in Equation 4.1. According to Brown et al. [24], an methanation plant efficiency of 80 % can be assumed for the year 2035. The efficiency of the electrolyzer is assumed to be 80 % by 2035 [24].

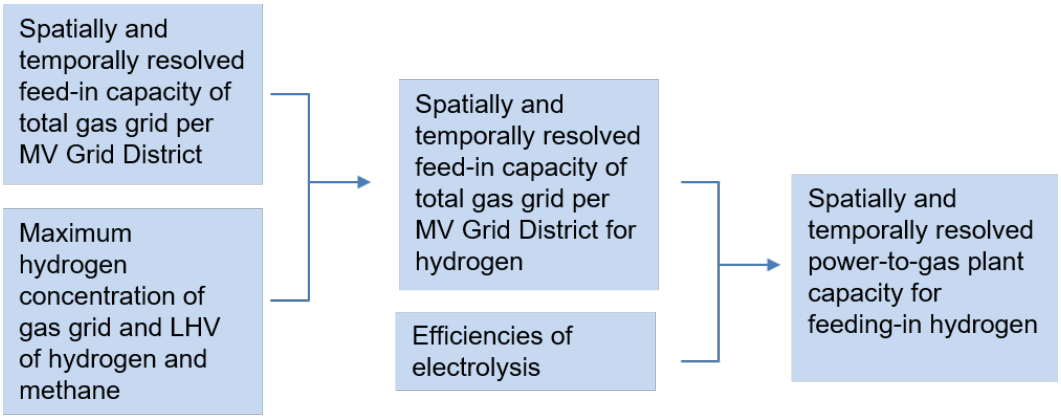

Figure 4.10: Power-to-gas plant capacity for hydrogen procedure

Figure 4.10 shows the procedure of determining the PtG plant capacity for injecting hydrogen into the gas grid. The capacity of electrolyzers is obtained in a similar way. However, the maximum feed-in concentration of hydrogen in the gas grid must be taken into account first. According to Hüttenrauch et al. [7], it is assumed that a maximum concentration of 5 vol.% hydrogen is permitted. An increase of the maximum concentration in the coming years is conceivable. In this context, 15 % is often discussed. For this reason, the feed-in capacity is also determined for a maximum concentration of 15 %. First, the volume flow $\dot{V}$ is determined by Equations 4.3 using the lower heating values (LHVs) of hydrogen and methane:

$$\dot{Q}_{th} = \dot{V} \cdot (l_{H_2} \cdot Hu_{H_2} + (1 - l_{H_2}) \cdot Hu_{CH_4}) \tag{4.3}$$

where $\dot{Q}_{th}$ is the feed-in capacity of the gas grid for injecting methane, l_{H_2} is the maximum concentration of hydrogen, Hu_{H_2} and Hu_{CH_4} represent the LHVs of hydrogen and methane. Subsequently, the feed-in capacity of hydrogen into the gas grid can be calculated using Equation 4.4:

$$\dot{Q}_{H_2} = l_{H_2} \cdot \dot{V} \cdot Hu_{H_2} \tag{4.4}$$

where $\dot{Q}_{H_2}$ represents the feed-in capacity of hydrogen. Using the calculated feed-in capacity of hydrogen and the efficiency of the electrolyzer, the capacity of the electrolyzer can be determined by Equation 4.5:

$$P_{el,electrolyzer} = \frac{\dot{Q}_{H_2}}{\eta_{electolyzer}} \tag{4.5}$$

where $P_{el,electrolyzer}$ stands for the capacity of the electrolyzer, $\dot{Q}_{H_2}$ is the feed-in capacity of hydrogen, and $\eta_{electolyzer}$ is the efficiency of the electrolyzer.

4.2.5 Determination of feed-in capacity of hydrogen at industrial sites

The network development plan [5] discusses building electrolyzers directly at industrial sites. In this way, the electrolyzers can simultaneously meet the hydrogen demand of the industry and provide flexibility to the electricity grid. The industry's natural gas demand is used to determine potential electrolyzer capacities at industrial sites. For the determination of this potential the natural gas demand of the industry sector at a spatial resolution of NUTS-3 is used. The data is provided by the LKD-EU study. The spatial and temporal resolution of the natural gas demand of the industry sector is carried out as described in the subsections 4.2.1 and 4.2.2. In order to adjust the natural gas demand to the hydrogen demand, a correction factor is developed. The correction factor takes into account the total annual hydrogen and natural gas demand of the industry, as determined by Equation 4.6:

$$f = \frac{Q_{H_2}}{Q_{CH_4}} \tag{4.6}$$

where Q_{H_2} is the total annual hydrogen demand and Q_{CH_4} is the total annual gas demand of the industry sector in Germany. According to [25] the total annual hydrogen demand of the industry sector by 2035 is set to:

$$Q_{H_2} = 78.5 \cdot 10^6 \text{ MW h} \tag{4.7}$$

The total annual gas demand of the industry sector in Germany is calculated from the data given by the LKD-EU study. The natural gas demand of the industry sector at NUTS-3 level is summed up for entire Germany.

The potential hydrogen demand of the industry sector is obtained by multiplying the spatially and temporally resolved gas demand by the correction factor. Since there is no limitation

by a maximum hydrogen concentration, the capacity of the electrolyzers can be determined directly by Equation 4.5.

4.3 eTraGo

The energy system model eTraGo[3] was developed within the research project open_eGo. The project can be divided into two basic sub-areas. An open database and platform for energy system modeling were developed. They were implemented in the form of the OpenEnergyPlatform (OEP) and the OpenEnergyDatabase (OEDB). Additionally, a planning tool for the determination of the optimal grid and storage expansion in Germany was developed. The planning tool electricity Grid optimization (eGo) contains of two energy system models respectively for transmission and distribution grid optimization using the open-source software Python for Power System Analysis (PyPSA). Figure 4.11 shows a schematic illustration of the eGo planning tool.

The aim of eTraGo is the economic optimization of transmission grid on the extra high voltage (EHV) and HV level including 380 kV, 220 kV and 110 kV grid with respect to grid and storage expansion. The energy system model electricity Distribution Grid optimization (eDisGo) optimizes the distribution grid level.

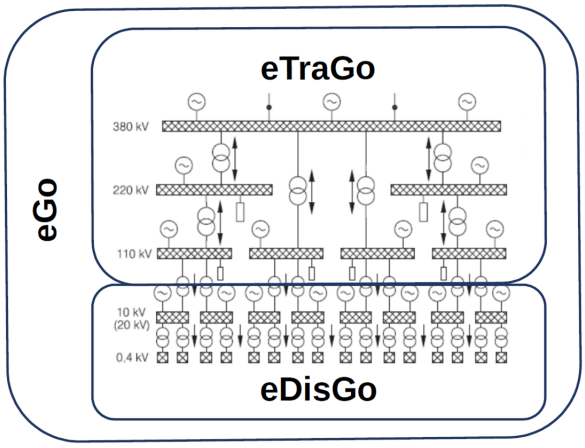

Figure 4.11: Planning tool eGo for the optimal grid and storage expansion in Germany divided into the energy system models eTraGo for optimizing the transmission grid and eDisGo for optimizing the distribution grid

[3] https://github.com/openego/eTraGo

eTraGo is discussed in more detail below. Figure 4.12 shows the steps of eTraGo for optimizing the transmission grid. The electricity grid model is imported from the OEDB and can be reduced to minimize computing time. For this purpose, spatial and temporal clustering methods are available. Subsequently, the linear optimal power flow (LOPF) calculation in PyPSA is performed, which includes the technical-economic optimization. The objective function is to minimize the total system costs. The results of optimizing EHV and HV grid level can either be evaluated with additional functions and plots or be passed as input variables of the cross-network tool eGo. The latter may require disaggregation of the results.

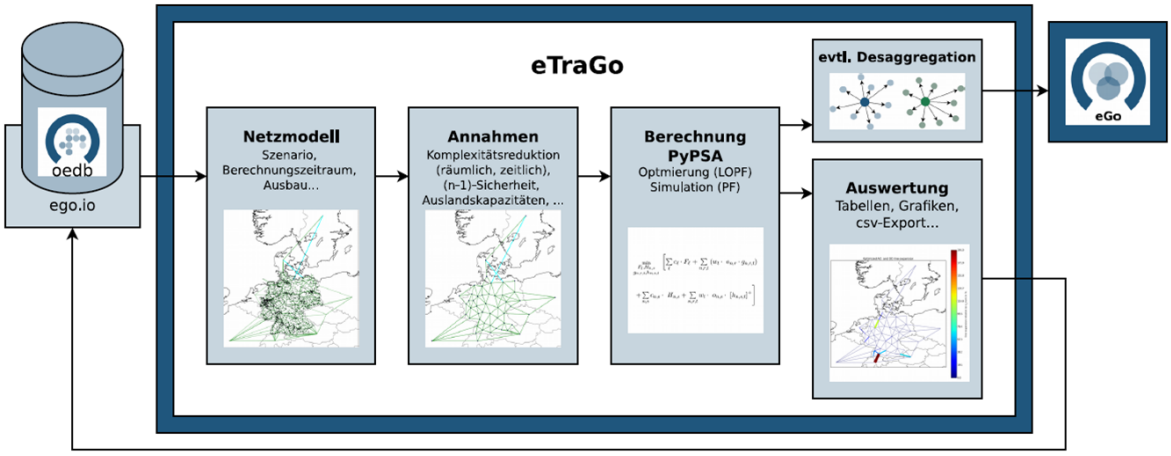

Figure 4.12: Schematic steps of eTraGo for the optimization of the transmission grid

For the modeling of the German transmission grid, the grid is divided into its voltage levels. These are called EHV, HV, MV, and low voltage (LV) and have voltage of $\geq 220\,\text{kV}$, 110 kV, 1 kV to 35 kV, and $< 1\,\text{kV}$ as shown in Figure 4.13. Electricity is transmitted between the adjacent voltage levels via substations. The transmission network is characterized by EHV and HV level and the substations in between. In addition, eTraGo also models the substations between HV and MV level, which represents the connection to the distribution grid. The distribution grid, which is calculated in eDisGo, is represented by MV and LV level.

In the project, geographical catchment areas were defined around the substations, in which the associated grid extends. The catchment area around the EHV-HV substation is called EHV Transmission Grid Area and the catchment area around the HV-MV substation is called MV Grid District. In eTraGo the transmission grid is represented by 424 EHV transmission grid areas and 3591 MV grid districts. The MV Grid Districts have an average

area of 99 km^2. The MV Grid Districts in eTraGo are well suited for the investigation and optimization of the allocation of PtG plants, because of the high spatial resolution and the key position between the transmission and distribution grid.

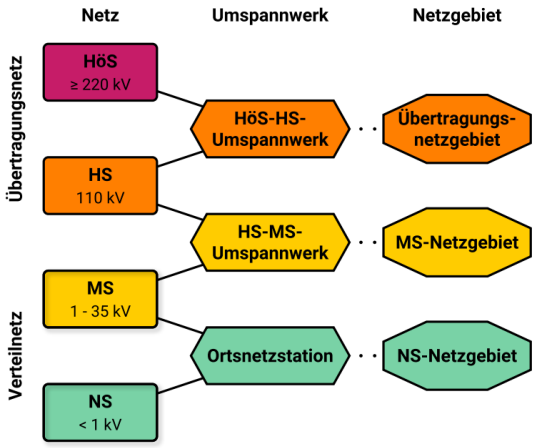

Figure 4.13: Electricity grid levels

4.3.1 Optimization method

Since eTraGo is based on the python tool PyPSA[4], the components introduced in PyPSA are also used to model the grid. The components relevant for this thesis are explained in Table 4.2.

For the optimization of the transmission grid, eTraGo is using the LOPF method of PyPSA. The goal of this method is to minimize the total annual costs, while the use of power plants under the given grid an market restrictions is modelled. If grid and storage expansion is permitted, their nominal power is an optimization variable and can be expanded in consideration of the annualized investment costs. The objective function is given by the following Equation 4.8:

Compliance with technical parameters is ensured by constraints for generators, storages, lines and transformers and Kirchoff's law. For detailed calculations of the constraints, please refer to the PyPSA documentation [35].

[4] https://pypsa.readthedocs.io/en/latest/index.html

Table 4.2: PyPSA Components

Component	Description
Network	Container for all components and functions within the network
Bus	Fundamental node where all associated objects are connected
Carrier	Energy carrier, such as solar, gas, wind, oil
Load	Energy consumer attaches to a single bus
Link	Component links two buses using a controllable directed flow with arbitrary energy carriers
Generator	Power generator converts energy from its carrier to the carrier-type of the bus to which it is attached
Store	The store is a fundamental component for storing energy and inherits its carrier from the bus it is connected to.

$$\min_{\substack{F_l, H_{n,s} \\ g_{n,r,t}, h_{n,s,t}}} \Bigg[\overbrace{\sum_{l} c_l \cdot F_l}^{\text{grid expansion}} + \overbrace{\sum_{n,r,t} (\omega_t \cdot o_{n,r} \cdot g_{n,r,t})}^{\text{generation variable costs}} + \underbrace{\sum_{n,s} c_{n,s} \cdot H_{n,s}}_{\text{storage expansion}} + \underbrace{\sum_{n,s,t} \omega_t \cdot o_{n,s} \cdot [h_{n,s,t}]^+}_{\text{storage variable cost}} \Bigg] \tag{4.8}$$

l:	Index line/transformer	$o_{n,r}$:	marginal costs of dispatch generator n, r
n:	Index bus		
r:	Index generator	$g_{n,r,t}$:	dispatch of generator n, r, t
t:	Index time step	$c_{n,s}$:	capital cost of storage n, s
s:	Index storage	$H_{n,s}$:	nominal capacity of storage n, s
c_l:	Capital cost of line/transformer l	$o_{n,s}$:	marginal costs of storage n, s
F_l:	Capacity of line/transformer l	$[h_{n,s,t}]^+$:	positive part of storage dispatch n, s, t
ω_t:	Weighting of time step t		

4.4 Integration of Power-to-Gas feed-in capacities into the power grid model eTraGo

In this section the integration of the PtG feed-in capacities into the power grid model eTraGo is discussed. The model is extended by three buses, each representing a part of

the network development plan. The buses serve as starting point for integrating the feed-in capacities. The first bus is called hydrogen grid-oriented and is used for the integration of the grid oriented electrolyzers. The second bus is called hydrogen industrial sites and is responsible for the integration of the electrolyzers at industrial sites. The third bus is called methane and represents the integration of the electrolyzers and methanation plant for feeding-in methane into the gas grid. Each electric bus is connected with each of the three gas buses using links, as shown in Figure 4.14. Within the eTraGo model, these links represent the PtG plants. Each gas bus is connected to a load and a store. As in all three cases the method chosen for integration is the same, only the integration of the PtG plants of the gas bus $H_2, grid\text{-}oriented$ is discussed more in detail.

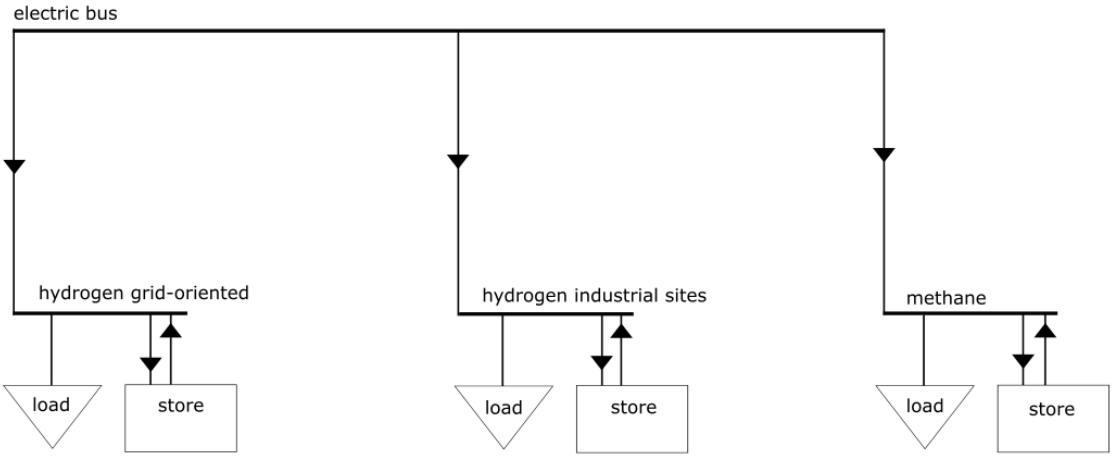

Figure 4.14: Integration of three additional gas buses into the eTraGo model including a load and a store per gas bus

In section 4.2.4, maximum installable PtG plant capacity and time series of the installable PtG plant capacity at each electric bus were determined. The gas bus is connected to each electric bus using a link. These links represent the PtG plants that can be built. In order to optimize the capacity of these, each link is assigned the minimum and maximum capacity of the PtG plant. The PtG plant capacity can be optimized between the minimum and maximum installable capacity:

$$\tilde{P}_n \leq P_n \leq \bar{P}_n \tag{4.9}$$

where $\tilde{P}_n$ is the minimum installable PtG plant capacity at bus n in [MW_{el}], P_n is the installed PtG plant capacity at bus n in [MW_{el}] and $\bar{P}_n$ is the maximum installable PtG

plant capacity at bus n in [MW_{el}]. The minimum installable PtG plant capacity is set to be 0.

$$\tilde{P}_n = 0\,\mathrm{MW_{el}} \tag{4.10}$$

Additionally, the links are assigned a normalized time series of the installable PtG plant capacity, which is derived from the time series determined in section 4.2.4. The time series is normalized to its maximum value.

$$P_{n,t,pu} = \frac{P_{n,t}}{P_{n,max}} \tag{4.11}$$

where $P_{n,t,pu}$ is the normalized PtG plant capacity at bus n at time step t in "per unit" $[-]$, $P_{n,t}$ is the PtG plant capacity at bus n and time step t and $P_{n,max}$ is the maximum PtG plant capacity at bus n.

The PtG plant dispatch $g_{n,t}$ at bus n is optimized but the installed PtG plant capacity P_n must not be exceeded at any time step t in the process. This results in the following constraint:

$$g_{n,t} \leq P_n * P_{n,t,pu} \tag{4.12}$$

All links are connected to the gas bus and feeding their product gas into it. In addition, a load and a storage are attached to the gas bus. The store is assigned a capacity. In case of the hydrogen grid-oriented PtG plants the capacity is included by setting the constraint:

$$E_{H_2,grid\text{-}oriented} = 37.5 \cdot 10^6 \mathrm{MWh_{th}} \tag{4.13}$$

where E_m is the storage capacity of the gas grid for hydrogen. The load is set to fulfill scenario C 2035 of the network development plan. The annual production of gas from the PtG plant must be:

$$E_{PtG,NEP,th} = P_{PtG,NEP} \cdot FLH_{PtG,NEP} \cdot \eta_{PtG} \tag{4.14}$$

where $E_{PtG,NEP,th}$ is the annual gas production by the PtG plants, $P_{PtG,NEP}$ defines the built PtG plant capacity in scenario C 2035 of the network development plan, $FLH_{PtG,NEP}$

defines the full load hours of the PtG plants in the same scenario and η_{PtG} is the efficiency of the PtG plants. In the case of the hydrogen grid-oriented PtG plant it results in:

$$E_{H_2,grid\text{-}oriented,NEP,th} = 3000\,\text{MW}_{\text{el}} \cdot 1500\,\text{h} \cdot 0.8 = 3.6 \cdot 10^6 \text{MWh}_{\text{th}} \tag{4.15}$$

An annual average production capacity of the gas produced by PtG plant can be derived by dividing $E_{PtG,NEP}$ by 8760 h:

$$P_{PtG,NEP,th} = \frac{E_{PtG,th}}{8760\,\text{h}} \tag{4.16}$$

The load to set is derived using the required annual average gas production $P_{PtG,NEP,th}$ and a normalized time series. The normalized time series is derived by averaging of the time series of PtG capacity determined in section 4.2.4 over all buses and normalizing by its mean value. This results in the load:

$$d_{PtG,t,th} = P_{t,pu,mean} \cdot P_{PtG,NEP,th} \tag{4.17}$$

where $d_{PtG,n,t,th}$ is the PtG load at time step t in [MW_{th}], $P_{t,pu,mean}$ is the normalized time series at time step t in "per unit" [-] and $P_{PtG,NEP,th}$ is the annual average gas production of the PtG plant in [MW].

All the gas produced by the PtG plants via the links is fed into the gas bus. The injected gas is used to cover the gas demand represented by the load. The difference is compensated using the storage:

$$g_{PtG,t,th} = \sum_n g_{PtG,n,t,th} = d_{PtG,t,th} + d_{PtG\text{-}storage,t,th} \tag{4.18}$$

where $g_{PtG,t,th}$ is the sum of gas produced by all PtG plants at time step t in [MW], $g_{PtG,n,t,th}$ is the gas produced by the PtG plant at bus n at time step t, $d_{PtG,t,th}$ represents the demand of gas from the load at time step t and $d_{PtG\text{-}store,t,th}$ is the demand of the store at time t.

According to [24] the investment cost of each PtG plant is:

$$c_{H_2,grid\text{-}oriented} = 350\,000\,€/\text{MW}_{\text{el}} \tag{4.19}$$

Table 4.3 shows the parameter for integrating all three types of PtG plant and its operation.

Table 4.3: Parameter for the integration of the PtG plant capacities

Parameter	$H_2, grid\text{-}oriented$	$H_2, industrial sites$	$methane$
P_{NEP}	3000 MW_{el}	4500 MW_{el}	500 MW_{el}
FLH_{NEP}	1500 h	3500 h	1000 h
E_{store}	$37.5 \cdot 10^6$ MW h	$37.5 \cdot 10^6$ MW h	$130 \cdot 10^6$ MW h
η	0.8	0.64	0.8
c	350 000 € MW^{-1}	350 000 € MW^{-1}	1 000 000 € MW^{-1}

4.5 Optimization of the Power-to-Gas plant allocation

From the previous sections, an energy system is obtained consisting of 3591 nodes and 8760 time steps. Computing time plays a decisive role in the optimization of large energy systems. Therefore, it is possible to cluster nodes in eTraGo. In this process the information of several nodes is combined in one node. As a result, the complexity of the energy system is reduced and the computing time is decreased. Another way to reduce the computing time is to choose a shorter time period to optimize. Both variants for minimizing the computing time are used in this thesis. It is determined to perform calculations over the entire year with 200 nodes and additional calculations with a higher resolution over a shorter time period.

In order to investigate the influences of the feed-in capacity of the gas grid on the allocation of PtG plants, different optimization cases are performed. Table 4.4 gives an overview on the different performed optimization cases. To be able to consider the temporal influence, calculations are carried out over different periods. All optimization cases are performed in accordance with the network development plan. Five calculations are carried out for the period of one week and one for an entire year. In the following paragraphs, the optimization cases are discussed in more detail.

The difference in the allocation of PtG plants between summer and winter is tested. To examine the seasonal impact, calculations are carried out for periods in summer with low gas

demand and in winter with high gas demand. In optimization case 1, the allocation of PtG plants is optimized for the week in summer with the lowest gas demand. For this, the time period is set to 4200 h to 4368 h. This optimization case follows the network development plan and all three gas buses are integrated. The gas bus $H_2, grid\text{-}oriented$ is provided with the capacities of the PtG plants feeding hydrogen into the gas grid. These capacities are determined in section 4.2.4 with an assumed maximum hydrogen concentration of 5 vol.% of the gas grid. The gas bus $H_2, industrialsites$ is provided with the capacities of the PtG plants located directly at the industrial sites, as determined in section 4.2.5. The gas bus $methane$ is provided with the capacities of the PtG plants feeding-in methane directly into the grid, as determined in section 4.2.4. To investigate the seasonal differences, optimization case 2 is executed with the same characteristics regarding the gas buses. The period with the highest gas demand in winter is selected. Thus, the time period is set to 1200 h to 1368 h.

The cases 3 to 5 are performed using the summer period because this period offers lower installable capacity. Therefore, the PtG plant capacities are not overestimated. In case 3, the influence of a higher installed capacity of PtG plants feeding hydrogen into the gas grid is investigated. Only the gas bus $H_2, grid\text{-}oriented$ is used for this purpose. The load attached to the gas bus is set to be 7500 MW_{el}.

The optimization case 4 examines the impact of a higher hydrogen feed-in limit concentration of the gas grid. This optimization is performed using the determined capacities of PtG plants feeding hydrogen into the gas grid. These capacities are calculated with a maximum feed-in concentration of 15 vol.%.

A reference calculation is carried out in order to determine the behaviour of the eTraGo model without the integration of the feed-in capacities. Hence, optimization case 5 is executed without the additional gas buses.

The last optimization case is used to determine the temporal influence over the course of the year. For this purpose, the calculation is performed without restricting the time period and is set to 1 h to 8760 h.

Table 4.4: Optimization cases

case	time period	number of nodes	H_2 grid-oriented	H_2 industrial sites	methane
1	4200 - 4368	400	P_{NEP} 3000 MW_{el} FLH_{NEP} 1500 h H_2-Limit 5 vol.%	P_{NEP} 4500 MW_{el} FLH_{NEP} 3500 h	P_{NEP} 500 MW_{el} FLH_{NEP} 1000 h
2	1200 - 1368	400	P_{NEP} 3000 MW_{el} FLH_{NEP} 1500 h H_2-Limit 5 vol.%	P_{NEP} 4500 MW_{el} FLH_{NEP} 3500 h	P_{NEP} 500 MW_{el} FLH_{NEP} 1000 h
3	4200 - 4368	400	P_{NEP} 7500 MW_{el} FLH_{NEP} 1500 h H_2-Limit 5 vol.%		
4	4200 - 4368	400	P_{NEP} 3000 MW_{el} FLH_{NEP} 1500 h H_2-Limit 15 vol.%		
5	4200 - 4368	400			
6	1 - 8760	100	P_{NEP} 3000 MW_{el} FLH_{NEP} 1500 h H_2-Limit 5 vol.%	P_{NEP} 4500 MW_{el} FLH_{NEP} 3500 h	P_{NEP} 500 MW_{el} FLH_{NEP} 1000 h

5 Results and Discussion

In this chapter, the results of the calculations carried out in this work are presented and discussed. The determined potential capacities of PtG plants feeding into the gas grid are illustrated. The results of optimizing the allocation of PtG pants are analyzed, and the influence of their potential capacities is evaluated.

5.1 Spatial distribution of the potential capacities of Power-to-Gas plants

In this section, the capacities determined for the PtG plants per MV Grid District are analyzed. In the following, only the maximum installable capacities of power-to-hydrogen plants that feed directly into the gas grid are discussed.

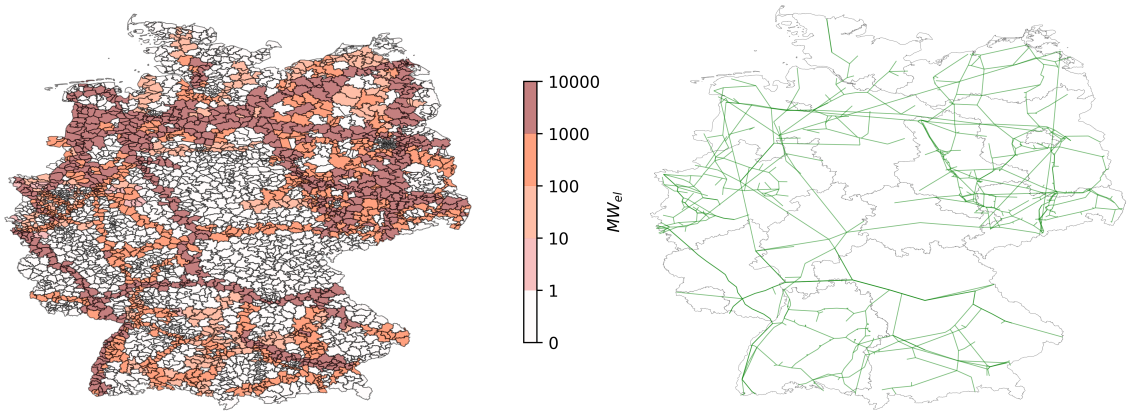

(a) Capacities per MV Grid District (b) Topology of the gas transmission grid

Figure 5.1: Maximum installable capacity of Power-to-Hydrogen plants per MV Grid District for feeding-in hydrogen at a maximum concentration of 5 vol.% into the gas transmission grid

Figure 5.1a shows the maximum installable capacity of power-to-hydrogen plants feeding into the gas transmission grid per MV Grid District. A maximum concentration of 5 vol.% hydrogen is applied. Figure 5.1b shows the transmission grid topology used to determine the capacities. Comparing the figures, the course of the pipelines through the MV Grid Districts can be clearly seen. The highest installable capacity of a MV Grid District is 8280 MW_{el}. A total of 1589 districts are crossed by pipelines. Thus, these MV Grid Districts provide an installable capacity of power-to-hydrogen plants feeding into the transmission grid. The MV Grid Districts with no pipelines have a capacity of 0 MW_{el}.

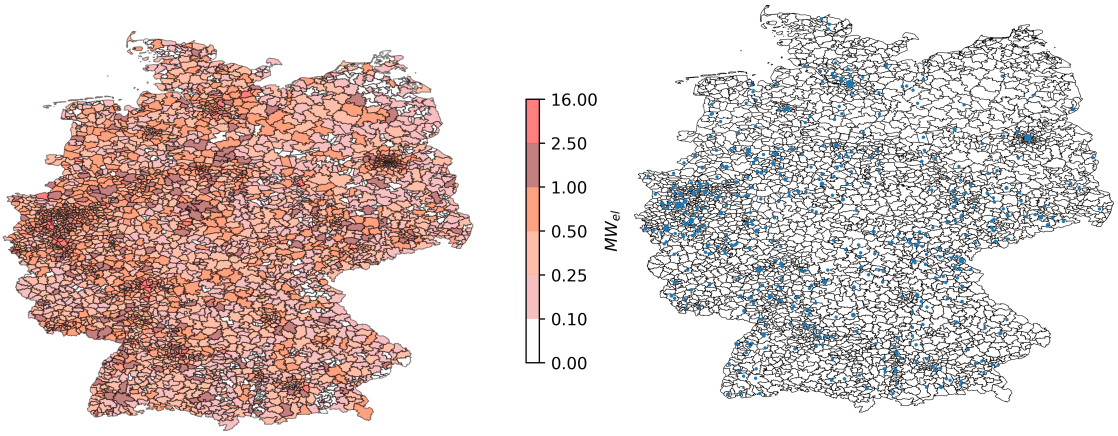

(a) Capacities per MV Grid District (b) Locations of industrial sites in Germany

Figure 5.2: Maximum installable capacity of PtG plants feeding hydrogen in the distribution grid per MV Grid District with a maximum hydrogen concentration of 5 vol.%

As described in subsection 4.2.1.2, the capacity of power-to-hydrogen plants feeding into the distribution grid is determined from the residual load between gas demand and gas production in each MV Grid District. Figure 5.2a shows the determined capacity of power-to-hydrogen plants feeding into the distribution grid. For the gas grid, a maximum hydrogen concentration of 5 vol.% is assumed. The installable capacity per MV Grid District is significantly lower than in the transmission grid. There are 3591 MV Grid Districts, as described in section 4.3. Only 339 MV Grid Districts have a maximum installable capacity of more than 1 MW_{el}; the remaining 3252 have a lower capacity. Figure 5.2b shows the energy-intensive industrial sites in Germany. The industry's gas demand influences the potential power-to-hydrogen capacity of 398 MV Grid Districts in Germany. A comparison of the figures clearly shows the influence of the industrial sites on the installable capacity of the power-to-hydrogen plants.

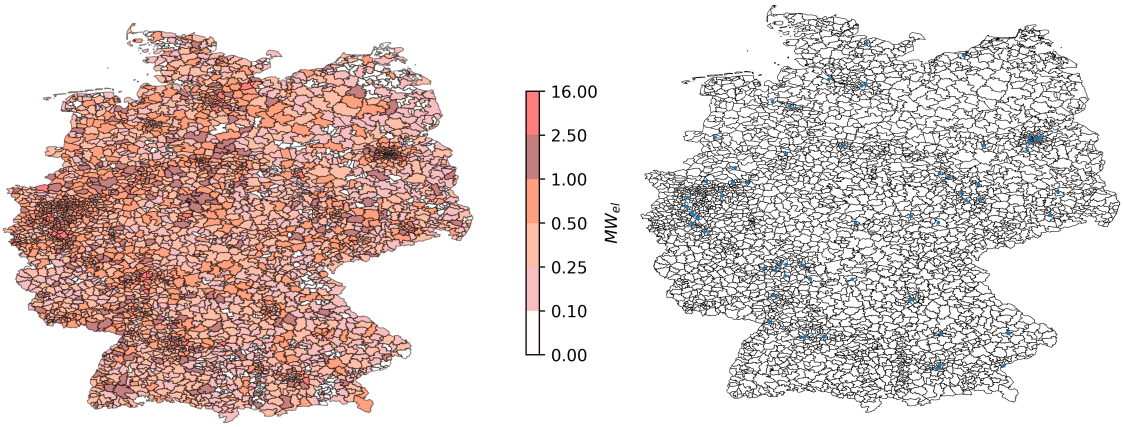

(a) Capacities per MV Grid District (b) Locations of gas-fired power plants

Figure 5.3: Maximum installable capacity of PtG plants feeding hydrogen in the distribution grid per MV Grid District with a maximum hydrogen concentration of 5 vol.%

But the MV Grid District providing the highest installable capacity are districts which contain gas-fired power plants. Figure 5.3 sets the capacities of power-to-hydrogen plants against the locations of gas-fired power plants. There are 47 MV Grid Districts containing gas-fired power plants.

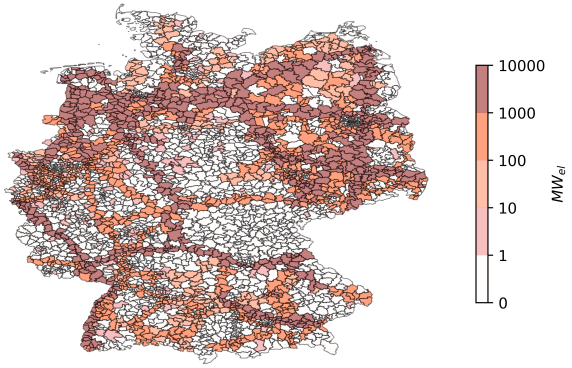

Figure 5.4: Maximum installable capacity of Power-to-Hydrogen plants per MV Grid District for feeding-in hydrogen at a maximum concentration of 5 vol.% into the entire gas grid

The potential capacity of the power-to-hydrogen plants for the entire gas grid is calculated from the sum of the capacities for the transmission grid and distribution grid. The results of this calculation are shown in Figure 5.4. Since the capacities determined from the distribution grid are low compared to the capacities determined from the transmission grid,

the distribution grid contributes much less to the distribution of large capacities than the transmission grid.

5.2 Temporal distribution of potential capacities of Power-to-Gas plants

This section discusses the results of the temporal distribution of the installable capacity of power-to-hydrogen plants. The methods described in section 4.2.2 are used to calculate the temporal distribution in the transmission grid and the distribution grid. In the following paragraphs, the results for power-to-hydrogen plants that feed directly into the gas grid are discussed more in detail. Just as in the case of the spatial distribution, the results with a maximum concentration of 5 vol.% hydrogen in the gas grid are addressed.

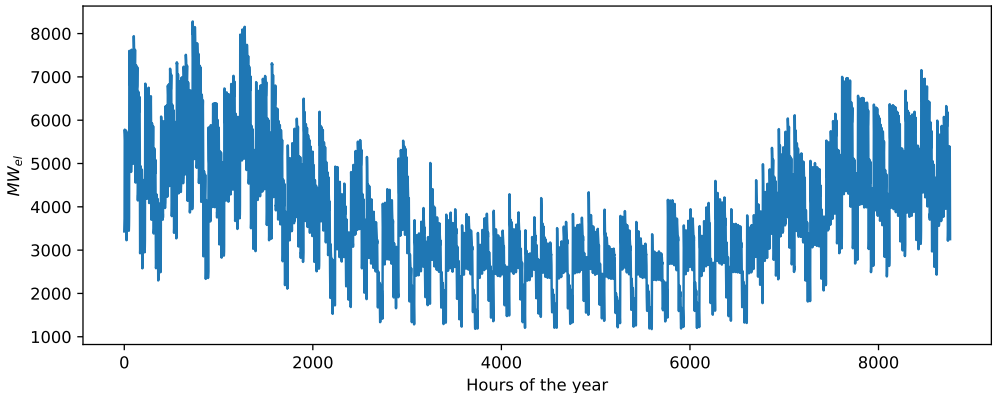

(a) Over the course of the year 2035

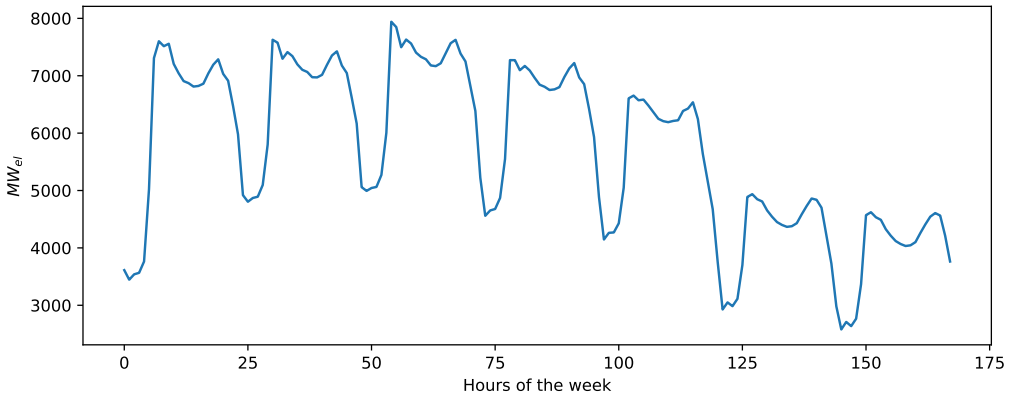

(b) Over the course of the first week of the year 2035

Figure 5.5: Time series of the installable power-to-hydrogen plant capacity in a MV Grid District for the transmission grid

The installable capacity for the gas transmission grid is temporally resolved using load

profile based on temperature-related gas demand. Figure 5.5 shows the time series of the installable capacity of power-to-hydrogen plant feeding into the transmission grid for the MV Grid District with the highest installable capacity. While Figure 5.5a shows the installable capacity over the course of the year 2035, Figure 5.5b shows the installable capacity over the course of the first week of 2035, beginning with a Monday.

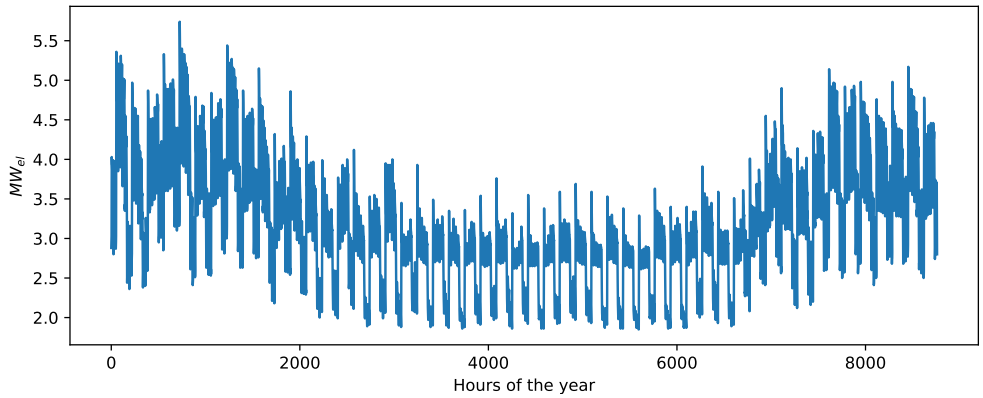

(a) Over the course of the year 2035

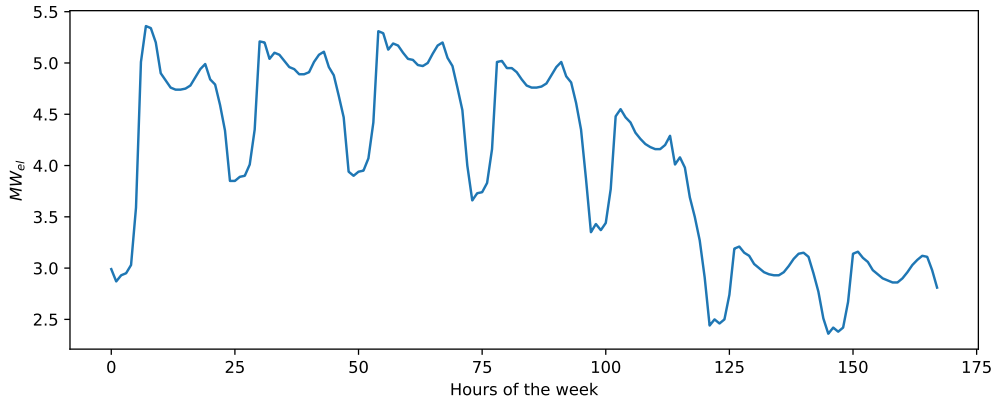

(b) Over the course of the first week of the year 2035

Figure 5.6: Time series of the installable capacity of a power-to-hydrogen plant feeding into the distribution grid for a MV Grid District consisting of households and industrial sites but no gas-fired power plants

The installable capacity fluctuates over the course of the year. The time series shows that the installable capacity decreases significantly in the summer months. In winter, the illustrated MV Grid District provides up to 8000 MW_{el}, while in summer it only provides around 3000 MW_{el}. On working days a higher capacity is provided than on weekends. Furthermore, the installable capacity also fluctuates throughout the day. This means that

more gas can be fed in during the day than at night.

The installable capacity for the gas distribution grid is temporally resolved using sector-specific load profiles. Figure 5.6 shows the time series of the installable capacity of power-to-hydrogen plants feeding into the distribution grid for a MV Grid District over the course of the year 2035. This MV Grid District contains industrial sites and households but no gas-fired power plants. Similar to the transmission grid, the distribution grid also has a lower installable capacity in the summer months. The installable capacity varies from around 3 MW_{el} in summer up to 5 MW_{el} in winter. Due to the load profile of the industry sector, the installable capacity during working days is higher. The fluctuations between day and night can be attributed to the household sector.

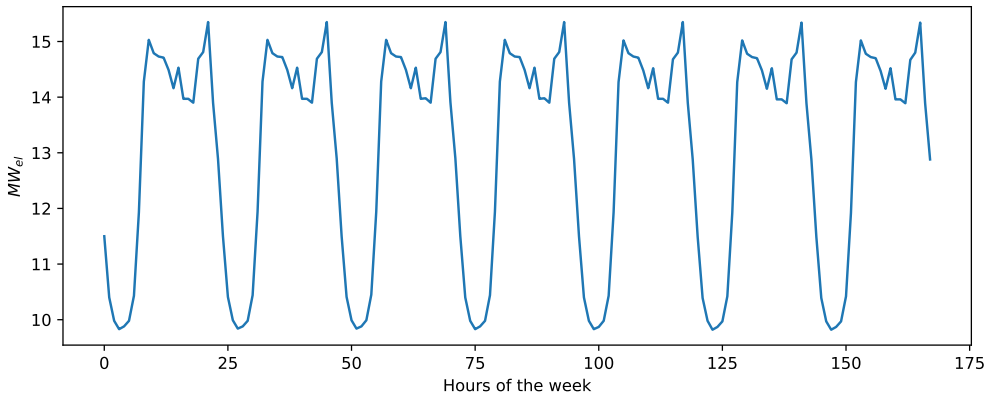

Figure 5.7: Time series of the installable power-to-hydrogen plant capacity feeding in the distribution grid for a MV Grid District consisting gas-fired power plants over the course of the first week of the year 2035

MV Grid District that also contain gas-fired power plants are dominated by the load profile of these power plants due to their high gas demand. Figure 5.7 shows the time series of the installable capacity of power-to-hydrogen plants for a MV Grid District, which also contains gas-fired power plants over the course of the first week of the year 2035. The installable capacity ranges between 10 MW_{el} at night and 15 MW_{el} during the day. In addition, fluctuations can be observed in the course of the day. However, no difference can be identified between working days and weekends as the influence of the industrial sites is negligible compared to the influence of the power plants.

Adding the installable capacities of power-to-hydrogen plants for transmission grid and distribution grid per MV Grid District forms the installable capacity of the entire gas grid. The effects on the temporal distribution are depicted in Figure 5.8 for a MV Grid District

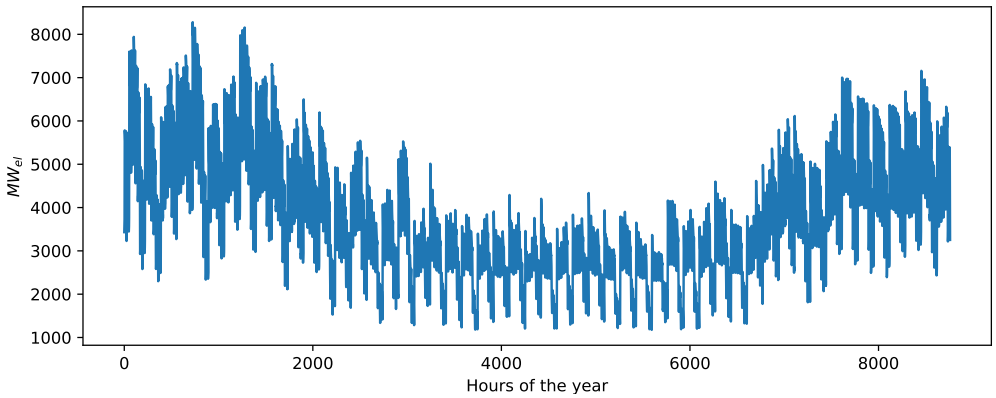

(a) Over the course of the year 2035

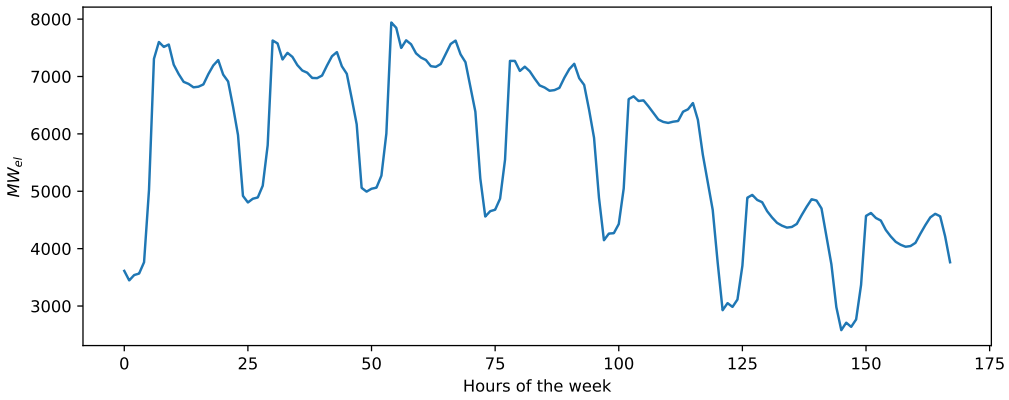

(b) Over the course of the first week of the year 2035

Figure 5.8: Time series of the installable power-to-hydrogen plant capacity including gas transmission grid and distribution grid for a MV Grid District

that includes both the transmission grid and the distribution grid. While 5.8a shows the installable capacity over the course of the year 2035, Figure 5.8b shows the capacity over the course of the first week of 2035. Due to the fact that the distribution grid provides a considerably lower capacity, the temporal distribution is significantly influenced by the transmission grid. It can be observed that the installable capacity decreases in summer. The installable capacity fluctuates over the course of the week between working days and weekends. There are also fluctuations between day and night.

5.3 Optimal allocation of Power-to-Gas plants in Germany

This section discusses the results of the six optimization cases performed. The results are obtained by applying the methods described in subsection 4.3.1. The characteristics of the individual optimization cases are described below. Since the calculation for the entire year must be calculated with a lower resolution of 100 nodes due to high computational time, calculations are also performed for the period of one week with a higher resolution.

In the first optimization case, all three gas buses are integrated. Thus, the optimization is performed for power-to-hydrogen plants feeding directly into the natural gas grid, power-to-hydrogen plants operating directly at industrial sites, and power-to-methane plants feeding into the natural gas grid. The optimization is carried out for a period of one week in summer. Figure 5.9 shows the optimal allocation of power-to-hydrogen plants used in a grid-oriented way and feeding directly into the natural gas grid.

The power lines of the power transmission grid are represented by the colored lines. The color bar indicates the loading of the corresponding power line in per unit of the maximum line capacity. The arrows indicate the direction of the electrical current. Each gray circle represents a power-to-hydrogen plant and the size of circle indicates the installed capacity of the plant. Most of the large power-to-hydrogen plants are built in northern Germany. Another large plant is installed in the Ruhr area.

In total, there are 22 power-to-hydrogen plants built. Figure 5.10 compares the installed capacity of power-to-hydrogen plants with the maximum installable capacity of the corresponding location in a bar plot. The orange bars indicate the maximum installable capacity, and the blue bars indicate the installed capacity at each node. On the x-axis, the corresponding nodes of the power-to-hydrogen plants are indicated. While Figure 5.10a shows the capacity of the five largest power-to-hydrogen plants built, Figure 5.10b shows the capacity of the 17 smaller power-to-hydrogen plants built. Except for the power-to-hydrogen plants at node 261 and 271, all plants are built with maximum installable capacity. The power-to-hydrogen plants have a capacity ranging from 1.24 MW_{el} up to 750 MW_{el}.

A closer look at node 261 with the largest installed power-to-hydrogen plant shows that here onshore wind power plants are installed with a capacity of 255 MW_{el}. This alone does not explain the installed capacity. Figure 5.9 shows that the power line connecting Sweden and Germany have a high relative loading. Taking a closer look at node 3, in the upper

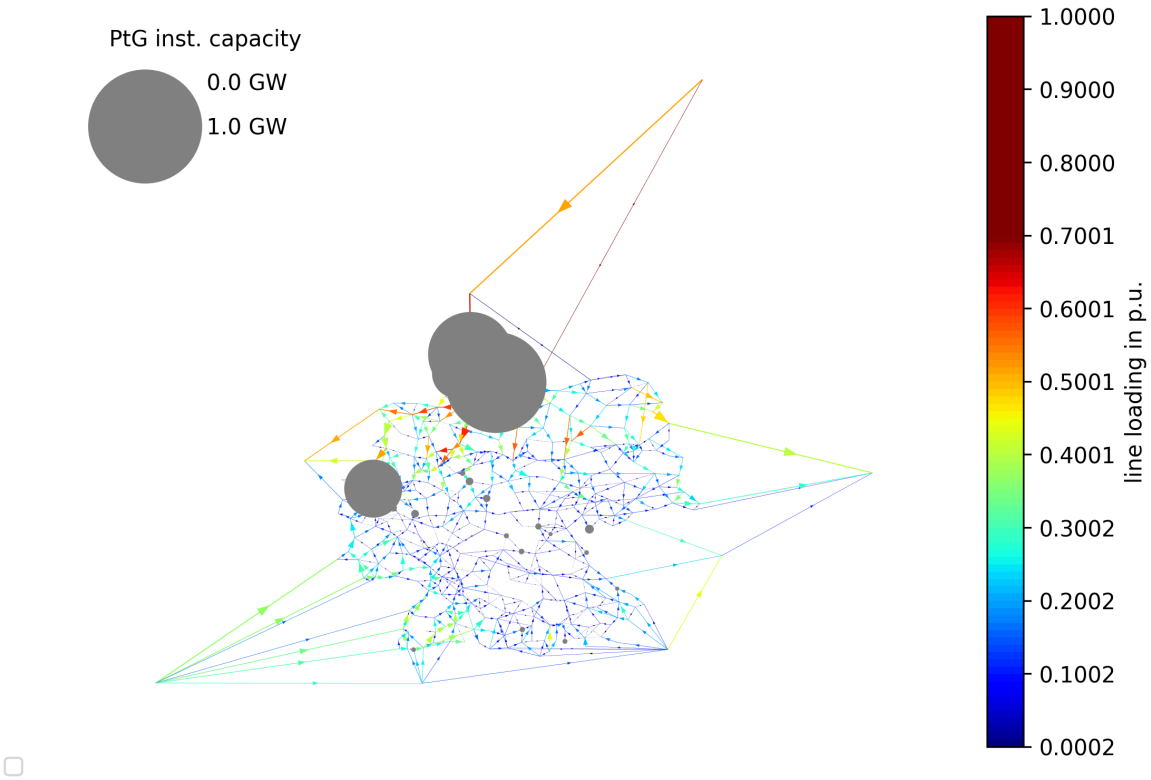

Figure 5.9: Allocation of grid-oriented power-to-hydrogen plants in Germany; the power lines are represented by the colored lines; the color bar indicates the loading of the power line in per unit of the maximum line capacity

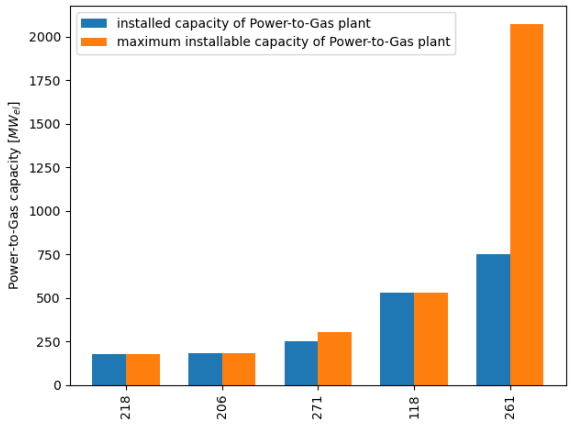

(a) Five largest power-to-hydrogen plants built

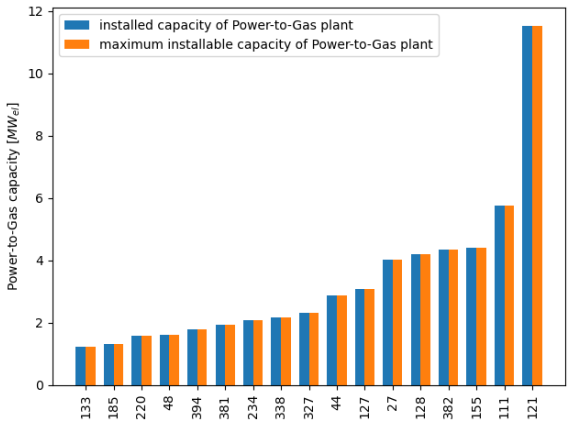

(b) 17 smaller power-to-hydrogen plants built

Figure 5.10: Installed capacity and maximum installable capacity of power-to-hydrogen plants used in a grid-oriented way in Germany

right corner, representing Sweden shows that here large wind power plants and hydroelectric power plants are installed.

The optimization case 1 also optimizes the allocation of power-to-hydrogen plants that supply industrial sites directly with hydrogen. Figure 5.11a shows the optimal allocation of power-to-hydrogen plants at industrial sites. A total of 78 power-to-hydrogen plants are built. The plants have an installed capacity in the range of 100 kW_{el} up to 487 MW_{el}. All power-to-hydrogen plants are built with the maximum installable capacity.

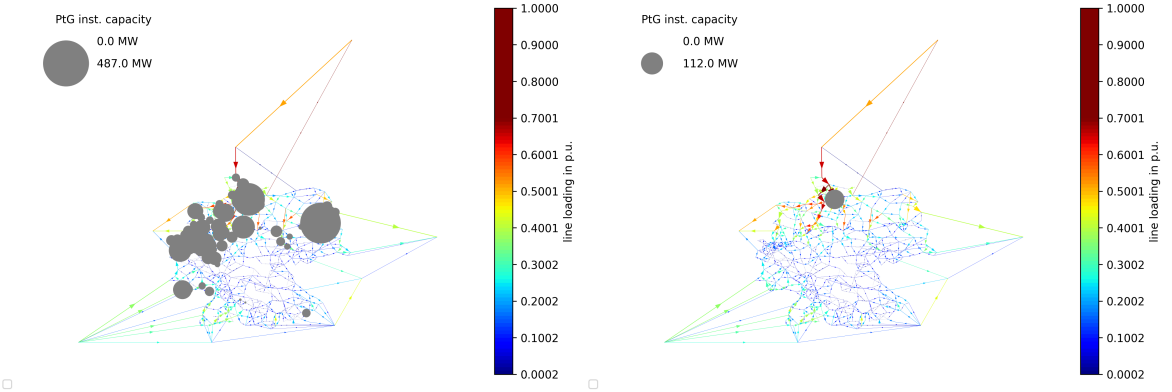

(a) Power-to-hydrogen plants at industrial sites (b) Power-to-methane plants

Figure 5.11: Allocation of power-to-gas plants in Germany, Results optimization case 1

The power-to-hydrogen plants are integrated exclusively in MV Grid Districts that also have industrial sites. The plants are mainly built in the northwest of Germany, where they take electricity from RES. In optimization case 1, power-to-methane plants are also built. Figure 5.11b shows the allocation of installed power-to-methane plants. Only one plant is built in the north of Germany. This plant has a capacity of 112 MW_{el}. The constraints for this optimization are derived from scenario C 2035 of the network development plan. This scenario assumes a lower methane than hydrogen production. Therefore, only one power-to-methane plant is built.

To investigate the influence of the temporal distribution of installable capacity, the second optimization is carried out with the same characteristics for one week in winter. Figure 5.12 shows the results of the optimization for the different power-to-gas plants. Changes in the allocation of the power-to-gas plants can be observed. In this case, only one power-to-hydrogen plant is built feeding directly into the gas grid, as shown in Figure 5.12a. The power-to-hydrogen plant has an installed capacity of 848 MW_{el} and is located in the south of Germany. In winter, there is a higher gas demand and therefore a higher feed-in capacity

than in summer. Hence, the installed power-to-gas capacity must not be distributed among several plants.

Figure 5.12b shows the allocation of power-to-hydrogen plants located directly at industrial sites. A total of 53 plants are built with a capacity ranging from 5 MW_{el} to 487 MW_{el}. Like in the optimization case 1 all plants are built with the maximum installable capacity. The large power-to-hydrogen plants near Hamburg and in Berlin are also built in this case. However, larger plants are now also located in southern Germany.

Figure 5.12c shows the allocation of power-to-methane plants. Only one plant is installed with a capacity of 76 MW_{el}. The power-to-methane plant is built at the same node as the power-to-hydrogen plant that feeds into the gas grid. Overall, it can be stated that for the optimization case considering the winter week a shift of power-to-gas plants to the south occurs. One reason for this could be the lower outside temperature in winter in the south than in the north of Germany. This leads to a higher installable capacity in the South. Also, different amounts of RES fed into the grid are conceivable. A congestion in the power grid is prevented by the power-to-gas plants. But for reliable statements, the results have to be examined by further calculations.

The optimization cases 3 to 5 are all carried out for a period of one week in summer. This enables a comparison of these cases with the optimization case 1.

The optimization case 3 is used to investigate a slightly different scenario for 2035. In this scenario, it is assumed that in 2035 there is a total of 7 GW_{el} instead of 3 GW_{el} of installed capacity of power-to-hydrogen plants in Germany that all feed into the gas grid. Power-to-hydrogen plants at industrial sites and power-to-methane plants that feed directly into the gas grid are not taken into account.

Figure 5.13 shows the allocation of power-to-hydrogen plants used in a grid-oriented way and feeding directly into the gas grid. A total of 27 plants are built. These include 10 plants with a capacity of 100 MW_{el} to 1155 MW_{el} and 17 smaller plants with a capacity in the range of 1 MW_{el} to 15 MW_{el}. Compared to optimization case 1, more large plants with a capacity of more than 100 MW_{el} are built due to the overall higher total installed capacity in Germany. Most of the plants are located in the north of Germany. Since power-to-hydrogen plants at industrial sites and power-to-methane plants feeding directly into the gas grid are not taken into account the distribution is slightly different. Additional plants are built in the southwest of Germany.

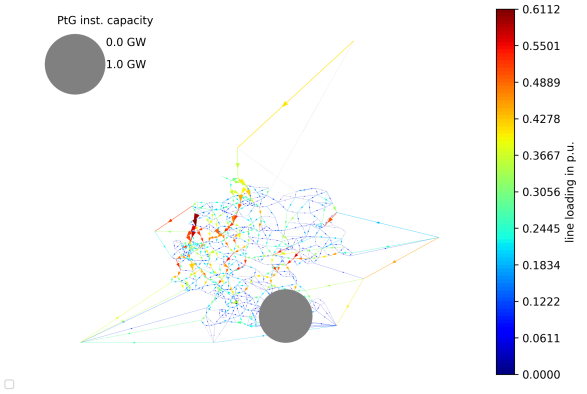

(a) Power-to-hydrogen plants feeding into the gas grid

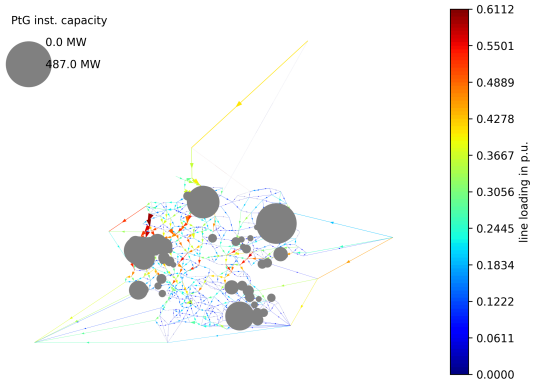

(b) Power-to-hydrogen plants at industrial sites

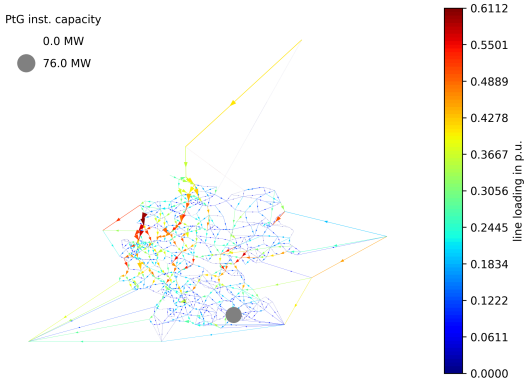

(c) Power-to-methane plants feeding into the gas grid

Figure 5.12: Allocation of power-to-gas plants in Germany in optimization case 2

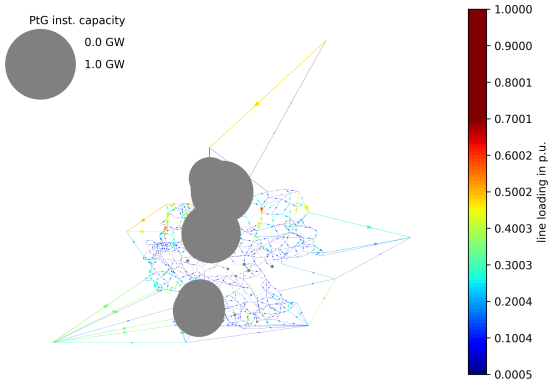

Figure 5.13: Allocation of power-to-hydrogen plants in Germany in optimization case 3

The optimization case 4 is used to investigate how a higher permitted hydrogen concentration in the gas grid affects the allocation of power-to-hydrogen plants. For this optimization, a permitted hydrogen concentration in the gas grid of 15 vol.% is applied instead of 5 vol.%. Power-to-hydrogen plants at industrial sites and power-to-methane plants are not taken into account by this optimization. Figure 5.14 shows the allocation of power-to-hydrogen plants that feed directly into the gas grid.

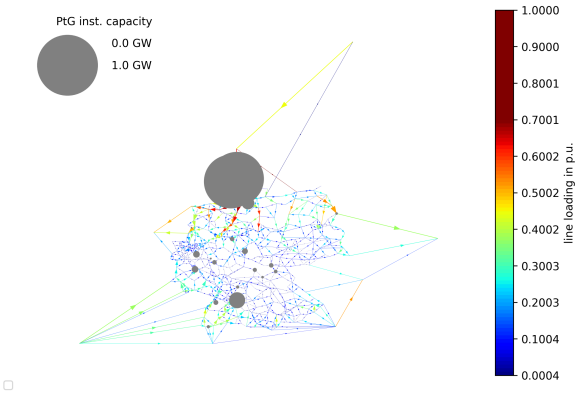

Figure 5.14: Allocation of power-to-hydrogen plants in Germany in optimization case 4

A total of 18 power-to-hydrogen plants are built, two of which stand out with a capacity of approximately 850 MW_{el}. The other plants have a capacity in the range of 1 MW_{el} to 75 MW_{el}. The two large plants with a capacity of approximately 850 MW_{el} are located in the north of Germany. As in the optimization case 1, they are operated with electricity imported from Sweden. The comparison with optimization case 1 shows that fewer but larger plants are built due to the higher installable capacity per MV Grid District. The higher installable capacity is achieved by increasing permitted hydrogen concentration to 15 vol.%.

The optimization case 5 is performed without the integration of power-to-gas plants. Figure 5.15 shows the power transmission grid without power-to-gas plants. The arrows indicate the direction of electrical current and the line color indicates the line loading. It can be clearly seen that the power lines in the north of Germany are exposed to high loads which can lead to congestions in the power grid. In the optimization cases that take power-to-gas plants into account, these plants are built to relieve the load on the power grid.

The optimization case 6 is carried out for a period of a year. In contrast to the previous optimization cases, the energy system is clustered to 100 nodes instead of 400. The construction of power-to-gas plants is also considered when optimizing the energy system.

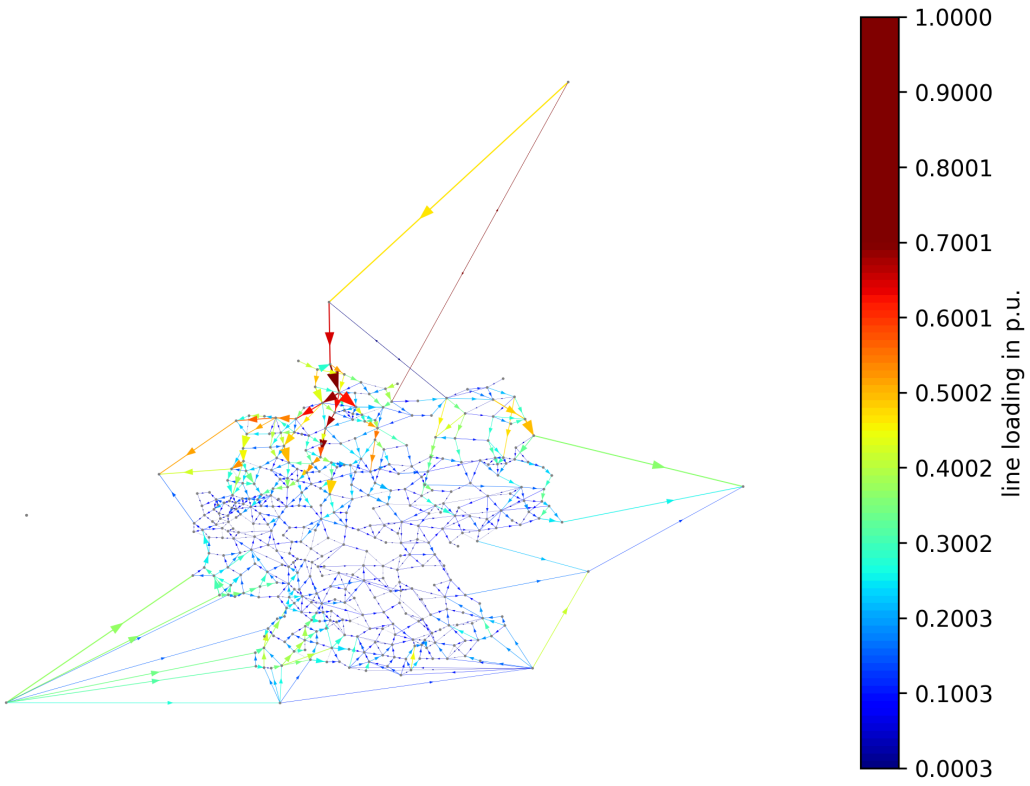

Figure 5.15: Power transmission grid without considering the construction of power-to-gas plants

By integrating all three gas buses, power-to-hydrogen plants that feed directly into the gas grid, power-to-hydrogen plants that are located directly at industrial sites and power-to-methane plants that feed directly into the gas grid can be built.

Figure 5.16 shows the allocation of power-to-hydrogen plants feeding into the gas grid and their installed capacity. Two power-to-hydrogen plants with a capacity of 454 MW_{el} and 887 MW_{el} are built in the north of Germany. While the plant at the node 86 is built with the maximum installable capacity, the plant at node 50 utilizes just 20 % of the maximum installable capacity. There are several electrical generators located at node 86. Here, the onshore wind power plants with an aggregated capacity of 6532 MW_{el} and the solar power plants with an aggregated capacity of 1439 MW_{el} must be mentioned in particular. There also exist biomass, coal-fired, gas-fired and waste-fired power plants with a capacity ranging from 20 MW_{el} to 228 MW_{el} at this node. Due to the high proportion of fluctuating RES and the high installable capacity of power-to-hydrogen plants at node 86, a power-to-hydrogen plant is assumed to be built here. This also avoids congestions in the power grid.

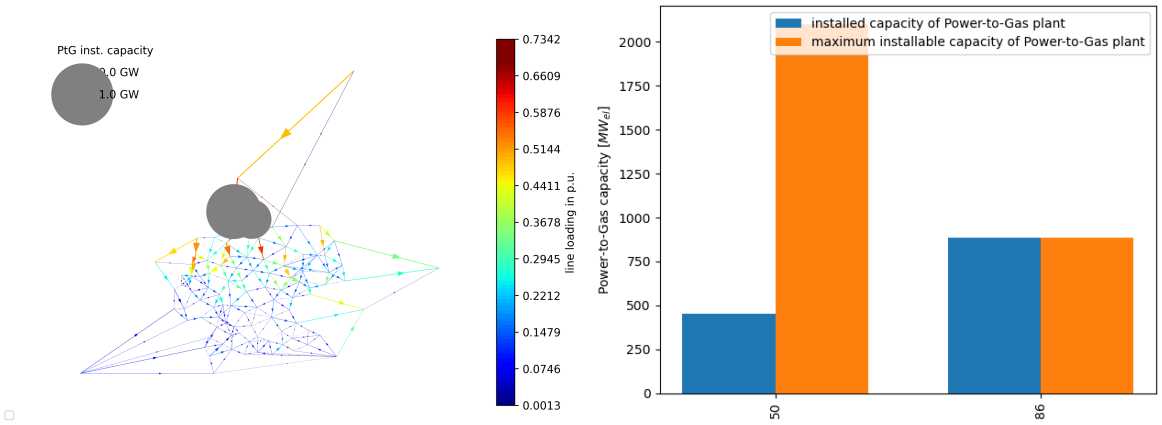

(a) Allocation of Power-to-hydrogen plants (b) Maximum installable and installed capacity

Figure 5.16: Allocation of power-to-hydrogen plants feeding into the gas grid and their installed capacity

Figure 5.17 shows the allocation of power-to-hydrogen plants located at industrial sites. While 5.17a shows the allocation of the plants, Figure 5.17b compares the maximum installable and the installed capacity of power-to-hydrogen plants. A total of 26 power-to-hydrogen plants are built directly at industrial sites. The plants are spread across industrial sites throughout Germany with a capacity of up to 486 MW_{el}. Figure 5.17b shows that most plants are built with the maximum installable power-to-hydrogen capacity of the MV Grid District.

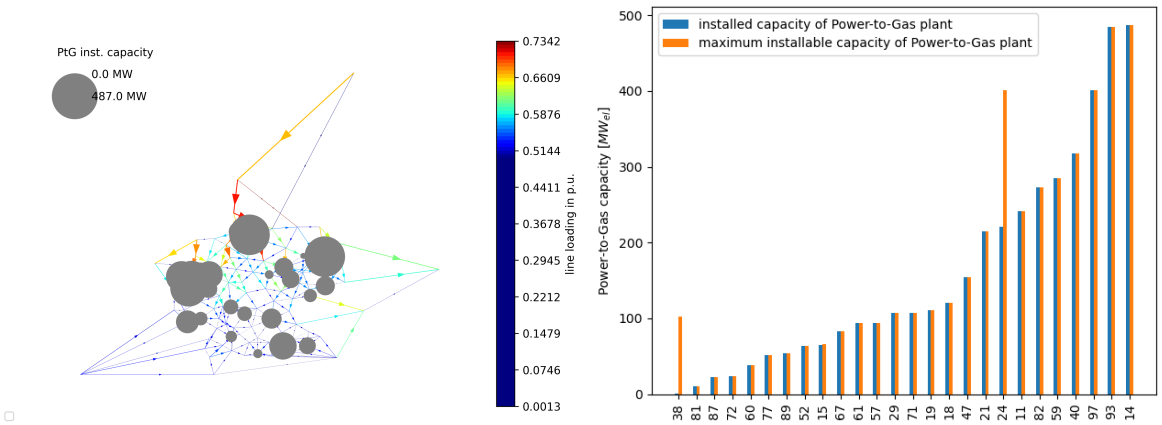

(a) Allocation of power-to-hydrogen plants (b) Maximum installable and installed capacity

Figure 5.17: Allocation of power-to-hydrogen plants located at industrial sites and their installed capacity

Figure 5.18 shows the allocation of power-to-methane plants. Only one power-to-methane

plant is built in the north of Germany. The plant is installed with a capacity of 120 MW_{el} at node 86. A comparison with Figure 5.16b shows that the largest power-to-hydrogen plant feeding into the gas grid is also built at node 86.

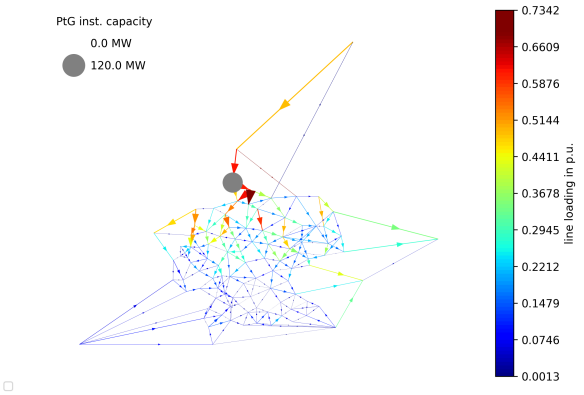

Figure 5.18: Allocation of power-to-methane plants feeding into the gas grid

6 Conclusion and Outlook

This chapter addresses the conclusion and gives an outlook on the next measures. The main component of this work is the determination of spatially and temporally resolved potential for installing power-to-gas plants in Germany. The potential is calculated based on the feed-in capacity of the gas grid. For the high spatial and temporal resolution, regionalization methods and load profiles are applied.

The integration of the installable power-to-gas capacity into the power grid model eTraGo allows for the calculation of the optimal distribution of power-to-gas plants. Six different optimization cases are calculated to demonstrate the usability of the determined data. The optimization cases are based on the scenario C 2035 of the network development plan. This allows statements to be made about the future expansion of power-to-gas plants, including the gas grid, with a high spatial and temporal resolution.

The first research question is investigated using all six performed optimization cases. The influence of the spatial distribution of the installable power-to-gas plant capacity can be explained using the different levels of installable capacity in the transmission grid and distribution grid. While the maximum installable capacity of power-to-hydrogen plants feeding into the transmission grid is on average 860 MW_{el} per MV Grid District, the maximum installable capacity of power-to-hydrogen plants feeding into the distribution grid is on average 1.5 MW_{el} per MV Grid District. As a result, power-to-gas plants feeding directly into the gas grid are mainly built in regions with transmission grid pipelines.

In order to answer the second research question, optimization cases 1 and 2 must be considered in more detail. Hereby, the influence of the temporal distribution of installable power-to-gas capacity is investigated. The temporal distribution of installable capacity also influences the allocation of power-to-gas plants. In optimization case 2, which is carried out for the period of one week in winter, the power-to-gas plants are increasingly built in the south of Germany. Due to the lower outdoor temperature in winter in the south than in the north, there is a higher gas demand and thus a higher feed-in potential for power-to-gas

plants. More detailed analyses of the results are required for an exact description of the effect.

The third research question is answered using optimization case 4. Here, the influence of a higher permitted hydrogen concentration in the gas grid on the allocation of power-to-hydrogen plants is investigated. A higher permitted hydrogen concentration leads to the construction of fewer power-to-gas plants but larger ones.

This work shows that the allocation of power-to-gas plants in the energy system strongly depends on the gas grid. The generated data set of spatially and temporally resolved installable capacity meets the requirements for the determination of the allocation of power-to-gas plants. Since the main part of this work is determining the potential power-to-gas plant capacity based on the gas grid, it is recommended to perform more optimizations in the future. It is also recommended to carry out the optimization with more nodes for the period of a year. Thus, the results can be evaluated reliably.

There are some limitations of the data presented. For accurate modeling of the gas grid, the gas flow must also be considered. Another limitation is how power-to-methane plants are integrated into the power grid model. Since power-to-methane consists of two process steps - electrolysis and methanation - such separated modeling is desirable.

The determined data set and the integration of the installable capacity of power-to-gas plants can serve as a starting point for further investigations. For example, enrichment of hydrogen in certain gas grid areas can be investigated.

Bibliography

[1] Fraunhofer ISE, "Energy-Charts," 2021.

[2] M. Robinius, A. Otto, P. Heuser, L. Welder, K. Syranidis, D. S. Ryberg, T. Grube, P. Markewitz, R. Peters, and D. Stolten, "Linking the power and transport sectors—Part 1: The principle of sector coupling," *Energies*, vol. 10, no. 7, p. 956, 2017.

[3] S. Schiebahn, T. Grube, M. Robinius, V. Tietze, B. Kumar, and D. Stolten, "Power to gas: Technological overview, systems analysis and economic assessment for a case study in germany," *International journal of hydrogen energy*, vol. 40, no. 12, pp. 4285–4294, 2015.

[4] M. Thema, F. Bauer, and M. Sterner, "Power-to-gas: Electrolysis and methanation status review," *Renewable and Sustainable Energy Reviews*, vol. 112, pp. 775–787, 2019.

[5] I. Posch and S. Mellahn, "Netzentwicklungsplan Gas 2020-2030 Szenariorahmen," 2019.

[6] F. Kunz, J. Weibezahn, P. Hauser, S. Heidari, W.-P. Schill, B. Felten, M. Kendziorski, M. Zech, J. Zepter, C. von Hirschhausen, D. Möst, and C. Weber, "Reference Data Set: Electricity, Heat, and Gas Sector Data for Modeling the German System," Dec. 2017.

[7] J. Hüttenrauch, G. Müller-Syring, H. Krause, W. Fichtner, C. Nolden, P. Hauser, T. Müller, D. Möst, P. Härtel, N. Gerhardt, *et al.*, "Integration fluktuierender erneuerbarer Energien durch konvergente Nutzung von Strom-und Gasnetzen-Konvergenz Strom-und Gasnetze (KonStGas): Abschlussbericht," 2018.

[8] J. Haumaier, P. Hauser, H. Hobbie, and D. Möst, "Grünes Gas für die Gaswirtschaft–Regionale Power-to-Gas-Potentiale aus Onshore-Windenergie in Deutschland," *Zeitschrift für Energiewirtschaft*, vol. 44, no. 2, pp. 61–83, 2020.

[9] S. B. (Destatis), "NUTS-Klassifikation," tech. rep., Statistisches Bundesamt, 2020.

[10] V. P. Z. H.-O. P. D. R. J. S. P. S. A. P. W. M.-O. C. P. R. P. S. C. J. M. Y. C. X. Z. M. G. E. L. T. M. M. T. Masson-Delmotte and T. W. (eds.), "Global Warming of 1.5°c. An IPCC Special Report on the impacts of global warming of 1.5°c above pre-industrial levels and related global greenhouse gas emission pathways, in the context of strengthening the global response to the threat of climate change, sustainable development, and efforts to eradicate poverty," 2018.

[11] P. Agreement, "Paris agreement," in *Report of the Conference of the Parties to the United Nations Framework Convention on Climate Change (21st Session, 2015: Paris). Retrived December*, vol. 4, p. 2017, HeinOnline, 2015.

[12] Umweltbundesamt, "Erneuerbare Energien in Deutschland Daten zur Entwicklung im Jahr 2019," tech. rep., Umweltbundesamt, 2020.

[13] B. für Wirtschaft und Energie, "Erneuerbare Energien in Zahlen," *Nationale und internationale Entwicklung im Jahr 2018*, 2019.

[14] D. P. Fekete, "Redispatch in Deutschland - Auswertung der Transparenzdaten April 2013 bis einschließlich September 2020," tech. rep., BDEW Bundesverband der Energie- und Wasserwirtschaft e.V., Reinhardtstraße 32 10117 Berlin, Nov. 2020.

[15] Bundesnetzsagentur, "Quartalsbericht Netz- und Systemsicherheit - Gesamtes Jahr 2019," tech. rep., Bundesnetzagentur, 2020.

[16] C. Pellinger and T. Schmid, "Verbundforschungsvorhaben Merit Order der Energiespeicherung im Jahr 2030. Teil 2: Technoökonomische Analyse funktionaler Energiespeicher," 2016.

[17] C. Brunner and T. Müller, "Kostenvergleich von unterschiedlichen Optionen zur Flexibilisierung des Energiesystems," *et Energiewirtschaftliche Tagesfragen*, vol. 65, no. 6, 2015.

[18] S. Milanzi, C. Spiller, B. Grosse, L. Hermann, J. Kochems, and J. Müller-Kirchenbauer, "Technischer Stand und Flexibilität des Power-to-Gas-Verfahrens," *With assistance of Joachim Müller-Kirchenbauer: TU Berlin, FG E&R. Available online at https://www. er. tu-berlin. de/fileadmin/a38331300/Dateien/Technischer_Stand_und_Flexibilit% C3% A4t_des_Power-to-Gas-Verfahrens. pdf*, 2018.

[19] M. Sterner and I. Stadler, *Energiespeicher-Bedarf, Technologien, Integration*. Springer-Verlag, 2014.

[20] M. Lehner, R. Tichler, H. Steinmüller, and M. Koppe, *Power-to-gas: Technology and business models*. Springer, 2014.

[21] A. Moser, J. Kellermann, M. Wahl, J. Schaffert, M. Zdrallek, D. Wolter, F. Möhrke, and J. Hüttenrauch, "Potenzialstudie von Power-to-Gas-Anlagen in deutschen Verteilungsnetzen," *Energie-, Wasser-Praxis*, vol. 2018, no. Januar, pp. 1–2, 2018.

[22] C. Brunner and J. Michaelis, "Wirtschaftliche Perspektiven für Power-to-Gas im zukünftigen Energiesystem," *ET. Energiewirtschaftliche Tagesfragen*, vol. 66, pp. 52–55, 03 2016.

[23] C. Golling, R. Heuke, H. Seidl, and J. Uhlig, "Roadmap Power to Gas; Baustein einer integrierten Energiewende," *Deutsche Energie-Agentur GmbH (dena), Berlin*, 2017.

[24] T. Brown, D. Schlachtberger, A. Kies, S. Schramm, and M. Greiner, "Synergies of sector coupling and transmission reinforcement in a cost-optimised, highly renewable European energy system," *Energy*, vol. 160, pp. 720–739, 2018.

[25] P. Nahmmacher, C. Paris, M. Ruge, S. Spieker, T. Anderski, S. Bohlen, R. Kaiser, C. Podewski, J. Apfelbeck, T. Kahl, F. Lukas, S. Sch¨fer, P.-S. Ganer, M. Muller, and D. St¨tzle, "Szenariorahmen zum Netzentwicklungsplan Strom 2035, Version 2021, Entwurf der Übertragungsnetzbetreiber," 2020.

[26] BMWi, "Die Nationale Wasserstoffstrategie," tech. rep., Bundesministerium für Wirtschaft und Energie (BMWi), June 2020.

[27] "Erdgas kann mehr. Wir auch. Gasinfrastruktur," tech. rep., VNG AG.

[28] N. Krzikalla, S. Achner, and S. Brühl, *Möglichkeiten zum Ausgleich fluktuierender Einspeisungen aus Erneuerbaren Energien: Studie im Auftrag des Bundesverbandes Erneuerbare Energie*. Ponte Press, 2013.

[29] S. von Roon, S. Pichlmaier, T. Hübner, T. Kern, and K. Ganz, "Studie zur Regionalisierung von PtG-Leistungen für den Szenariorahmen NEP 2020 - 2030," *FfE, München*, 2019.

[30] T. Estermann, S. Pichlmaier, A. Guminski, and C. Pellinger, "Kurzstudie Power-to-X–Ermittlung des Potenzials von PtX-Anwendungen für die Netzplanung der deutschen üNB," *FfE, München*, 2017.

[31] J. Michaelis, P. Hauser, and C. Brunner, "Die Einbindung von Power-to-Gas-Anlagen in den Gassektor," *Energiewirtschaftliche Tagesfragen, Bd*, vol. 66, pp. 8–12, 2016.

[32] A. Energiebilanzen, "Vorwort zu den Energiebilanzen für die Bundesrepublik Deutschland," 2008.

[33] D. Bothe, M. Janssen, S. Poel, and T. Eich, "Der Wert der Gasinfrastruktur für die Energiewende in Deutschland," *frontier economics et al., Tech. Rep.*, 2017.

[34] D. Schmidt, "NUTS-3 Regionalization of Industrial Load Shifting Potential in Germany using a Time-Resolved Model," Master's thesis, Carl von Ossietzky Universit¨at Oldenburg, 2019.

[35] T. Brown, J. Hörsch, and D. Schlachtberger, "PyPSA: Python for power system analysis," *arXiv preprint arXiv:1707.09913*, 2017.